Sea Grant College Program

STRUCTURAL MODELING OF THE TENSILE BEHAVIOR OF EIGHT-STRAND ROPES

Youjiang Wang
Stanley Backer
Department of Mechanical Engineering
Massachusetts Institute of Technology

MITSG 89-28

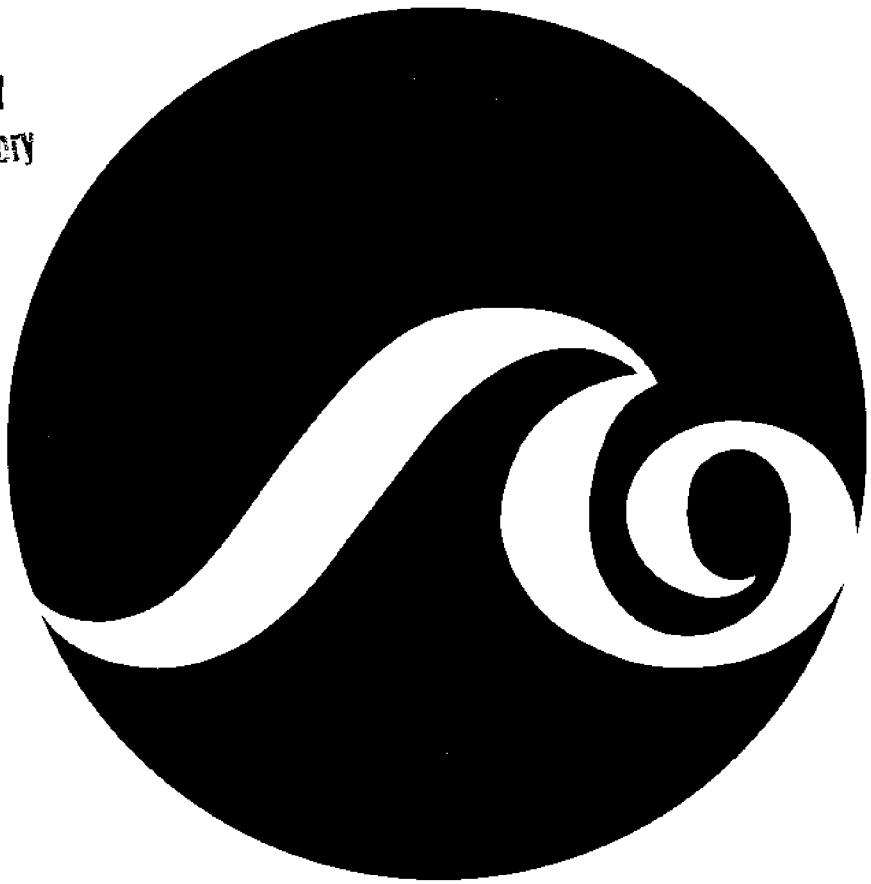

Massachusetts Institute
of Technology
Cambridge, Massachusetts
02139

STRUCTURAL MODELING OF THE TENSILE BEHAVIOR OF EIGHT-STRAND ROPES

Youjiang Wang
Stanley Backer
Department of Mechanical Engineering
Massachusetts Institute of Technology

MITSG 89-28

Sea Grant College Program
Massachusetts Institute of Technology
Cambridge, MA 02139

Grant No: NA86AA-D-SG089
Project No: RT-11

ABSTRACT

The tensile load-elongation behavior of eight-strand ropes has been studied by structural modelling in which the rope tensile load, interstrand pressures, and strand relative movements as functions of rope tensile strain are determined based on the rope geometries before and after deformation.

Contents

1 INTRODUCTION

Synthetic ropes are structures which offer flexibility and high tensile strength. They are widely used in many applications including marine towing and mooring. With the development of rope manufacturing technology, synthetic ropes are available in many structural types. Among them, three strand twisted, double braided, and eight strand plaited ropes are the most commonly used ones.

Eight strand plaited synthetic ropes have the advantages that no torque, and thus no rotation is induced when they are stretched, by virtue of their axial symmetric structures.

In order to study and characterize the mechanisms of rope deterioration, and to predict the mechanical behavior of eight strand ropes, it is necessary to develop valid models for the eight strand ropes under different loading conditions. Such models can provide useful information on rope construction parameters which give desired rope mechanical behavior. As the first step, the tensile load-elongation behavior of eight-strand ropes has been studied by a structural modelling in which the rope tensile load, interstrand pressures, and strand relative movements are determined as functions of rope tensile strain and based on the rope geometries before and after deformation.

2 GEOMETRY OF EIGHT-STRAND ROPES

2.1 Geometry of the Strand Axis

To facilitate the understanding of the structure of eight strand ropes, a short rope was made in the laboratory, using a small circular-cross-sectional double braided rope for each of the eight strands. Photographs of this rope and other two commercially made eight strand ropes are shown in Figure 1. By virtue of symmetry,

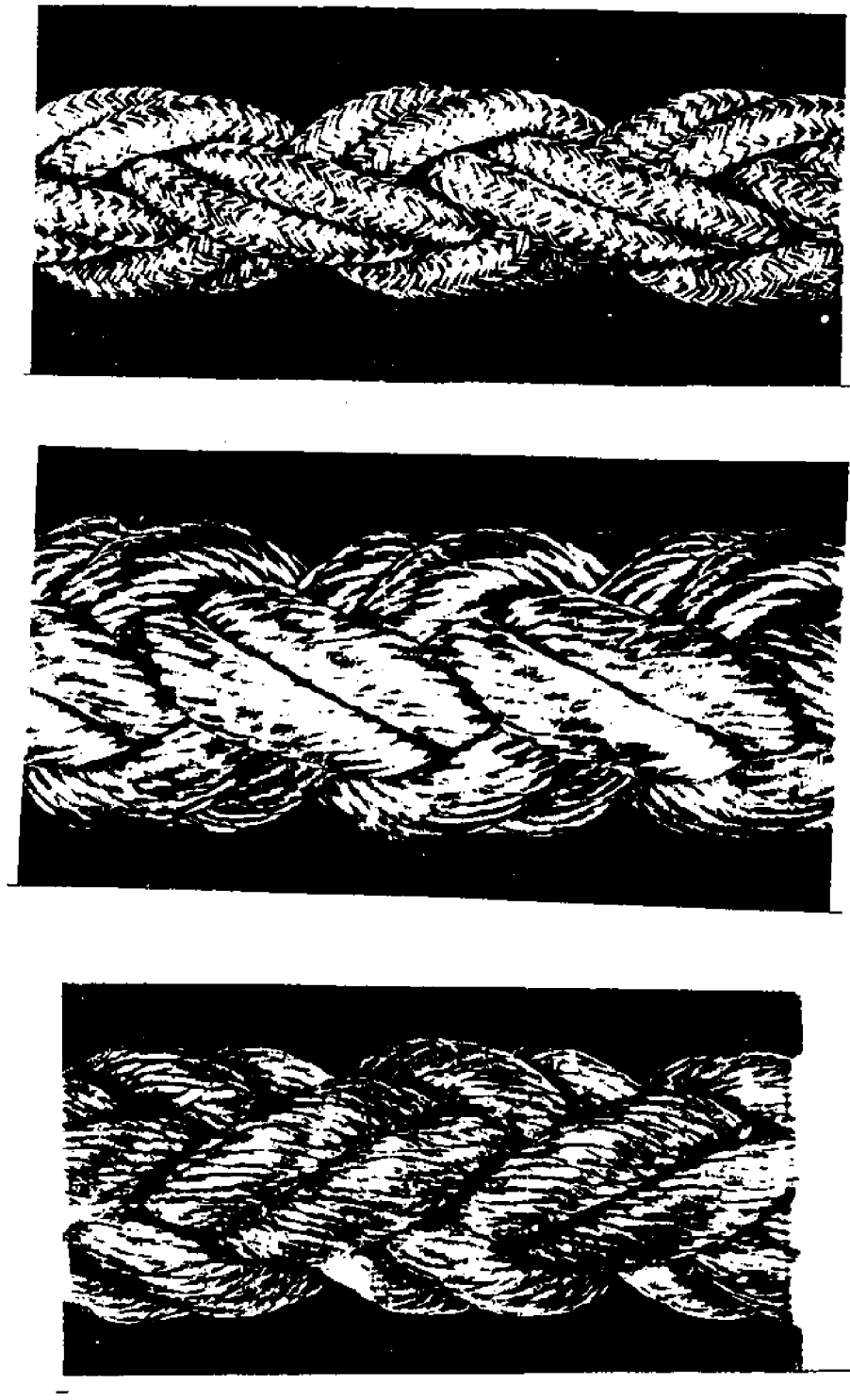

Figure 1: Photographs of eight strand ropes. (a) A hand-made structure, (b) A new rope, (c) A used rope

only one of the eight strands of each rope needs to be studied. In examination of the path of a single rope strand in a load-free state, it was noted that the projections of the strand axis on two perpendicular planes closely follow the wave form of sinusoidal curves, as illustrated in Figure 2. The sine waves on the two planes, XOZ and YOZ planes, both have the same period, but with different magnitudes and phase shifts. For the coordinates selected in Figure 2, the strand path for an unstretched eight-strand rope can be represented as:

$$X_s = X_{max} \sin \frac{2\pi(Z_s + B)}{H} \tag{1}$$

$$Y_s = Y_{max} \cos \frac{2\pi Z_s}{H} \tag{2}$$

where H is the length of one period of rope, X_{max}, Y_{max} are the maximum magnitude of X_s and Y_s, and B is the phase shift for X_s, which can be estimated from Figure 3 as

$$B = \frac{R_s}{\sin \alpha} \qquad \text{with} \qquad \tan \alpha = \left. \frac{\partial X_s}{\partial Z_s} \right|_{Z_s = -B} = \frac{2\pi}{H} X_{max} \tag{3}$$

where r_s is the radius of the strand.

When a rope is stretched at the two ends, the rope structure must adjust itself to satisfy two constraints:

- The boundary condition: the rope length multiplied by the rope strain must be equal to the rope stretch length; and
- The equilibrium condition: the total strand force components in the axial direction of the rope must remain constant along the rope.

As can be expected, when the rope is stretched the strand path functions become very complicated and may no longer be represented by the simple sinusoidal

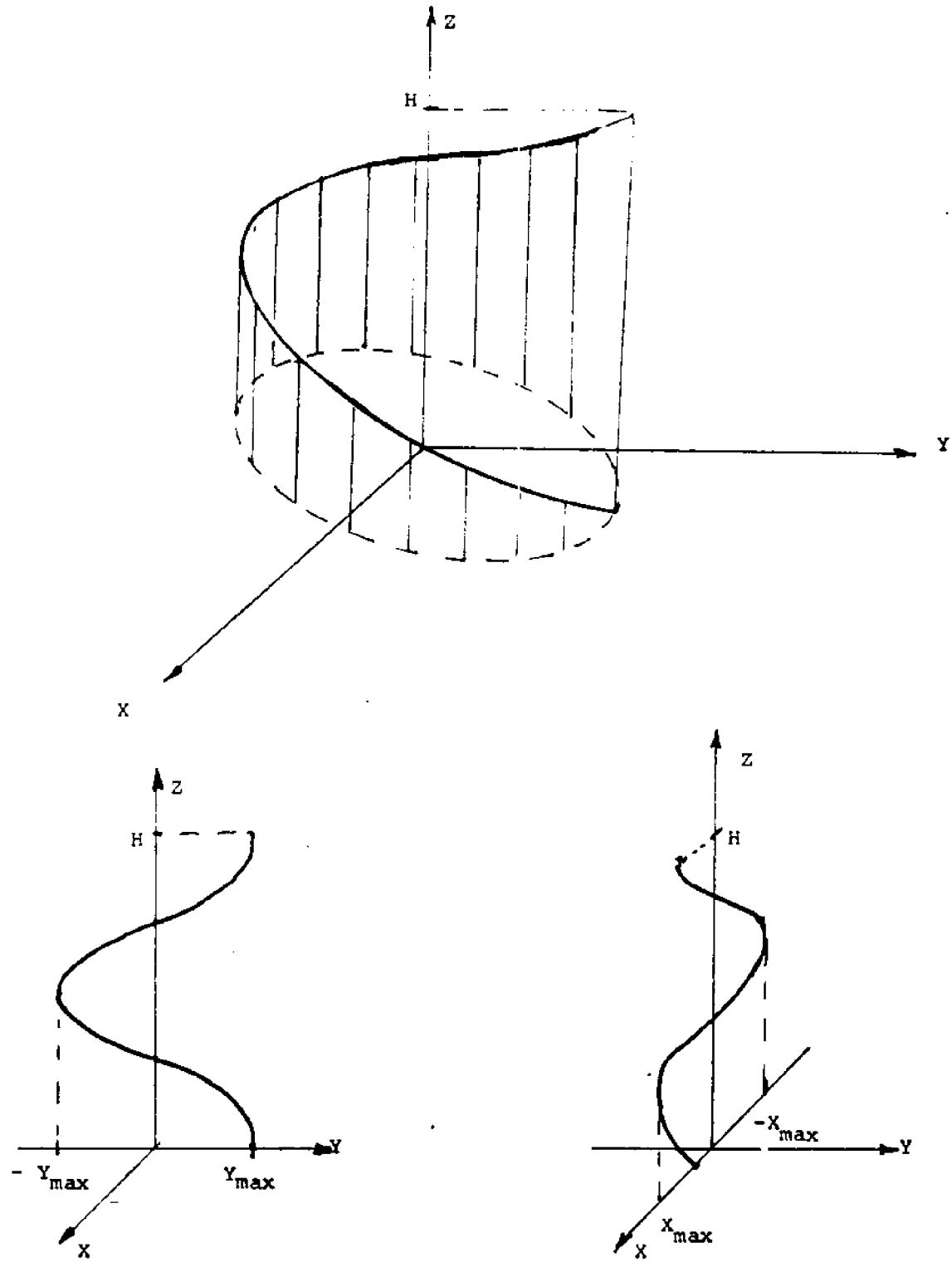

Figure 2: Geometry of rope strand axis

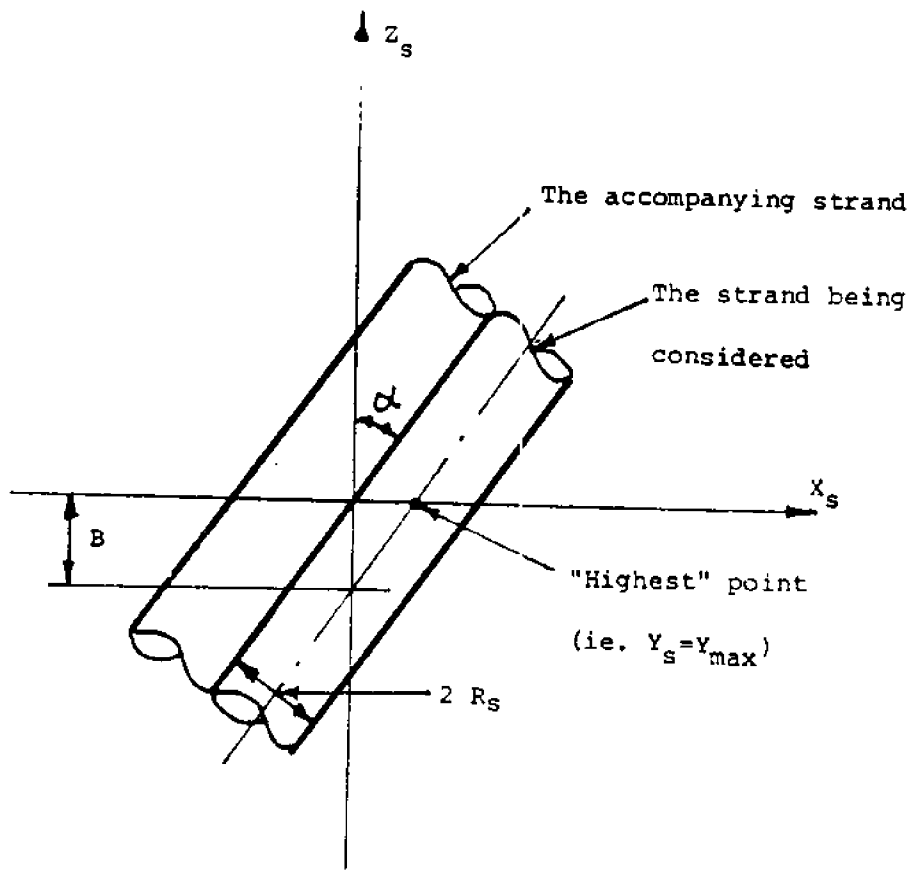

Figure 3: Determination of phase shift *B*

functions. One method of describing the stretched strand path is to use Fourier series representations, given as:

$$X_s = \int_{k=0}^{\infty} [B_k \sin(kAZ_s) + C_k \cos(kAZ_s)] \tag{4}$$

$$Y_s = \int_{k=0}^{\infty} [D_k \sin(kAZ_s) + E_k \cos(kAZ_s)] \tag{5}$$

where A, B_k, C_k, D_k, and E_k ($k = 0, 1, 2,...$) are functions of the rope strain, to be determined by the above two conditions. In practice, however, it is impossible to use infinite series to describe the strand path in the calculation. When using the first few terms in the series for X_s and Y_s, the higher frequency terms introduce undesirably high noise in the derivatives of X_s and Y_s functions, and thus this approach was found inappropriate.

The strand path functions used in this model are defined as follows

$$X_s(z) = X_{max} \sin \frac{2\pi(z + B)}{H} \tag{6}$$

$$Y_s(z) = Y_{max} \cos \frac{2\pi z}{H} \tag{7}$$

$$\frac{dZ_s}{dz} = 1 + \epsilon_a(z) \qquad \text{or} \qquad Z_s(z) = \int_0^z [1 + \epsilon_a(z)] dz \tag{8}$$

where z is the local coordinate of the strand axis fixes to the material points, and is directly related to the global axial coordinate Z_s by Eq 8, B is the phase shift given by Eq 3, H is the length of one period of rope at load-free state, and X_{max}, Y_{max}, and $\epsilon_a(z)$ are explained below.

In the strand path functions, X_{max} and Y_{max} are the magnitudes of the X_s and Y_s waves, determined from rope radius (r_r) and the strand radius (r_s), which in turn are functions of rope strain (ϵ_r) and rope lateral contraction ratio (μ):

$$X_{max}(\epsilon_r) = r_r(\epsilon_r) - 3r_s(\epsilon_r) \tag{9}$$

$$Y_{max}(\epsilon_r) = r_r(\epsilon_r) - r_s(\epsilon_r) \tag{10}$$

$$r_r(\epsilon_r) = (1 - \mu\epsilon_r)\, r_{r0} \tag{11}$$

$$r_s(\epsilon_r) = (1 - \mu\epsilon_r)\, r_{s0} \tag{12}$$

Where r_{r0} and r_{s0} are rope and strand radii at load-free state respectively. In Eq 12 the strand is assumed to have the same relative amount of lateral contraction as the rope structure does, but in reality one may expect that the rope and the strands contract differently when stretched. The lateral contraction ratio (μ) for rope structures has been observed to be within the range of 0.3 to 1.0, varying with rope strain level and rope structures. In this model, two forms of lateral contraction ratio expressions are used:

1. constant μ: e.g.: μ= 0.3, or μ= 0.6;

2. μ as an exponential function of rope strain:

$$\mu = \mu_0 e^{-\epsilon_r/\epsilon_0}$$

where μ_0 is the initial lateral contraction ratio and ϵ_0 is a constant.

$\epsilon_a(z)$ in the strand path functions (Eq 8) is the "axial strain" as a function of rope strain (ϵ_r) and axial position (z). It is determined by the model from equilibrium and boundary conditions. To help understand the definition of this axial strain $\epsilon_a(z)$, we consider stretching one rope period on which some lines were drawn in the load-free state at constant intervals (Figure 4). In the load-free state, the parameter z is identical to the strand axial coordinate Z_s. But when the rope is stretched, the coordinate Z_s of a cross-section will change with the movement of the cross-section. However the parameter for that cross- section will not change, as z is associated

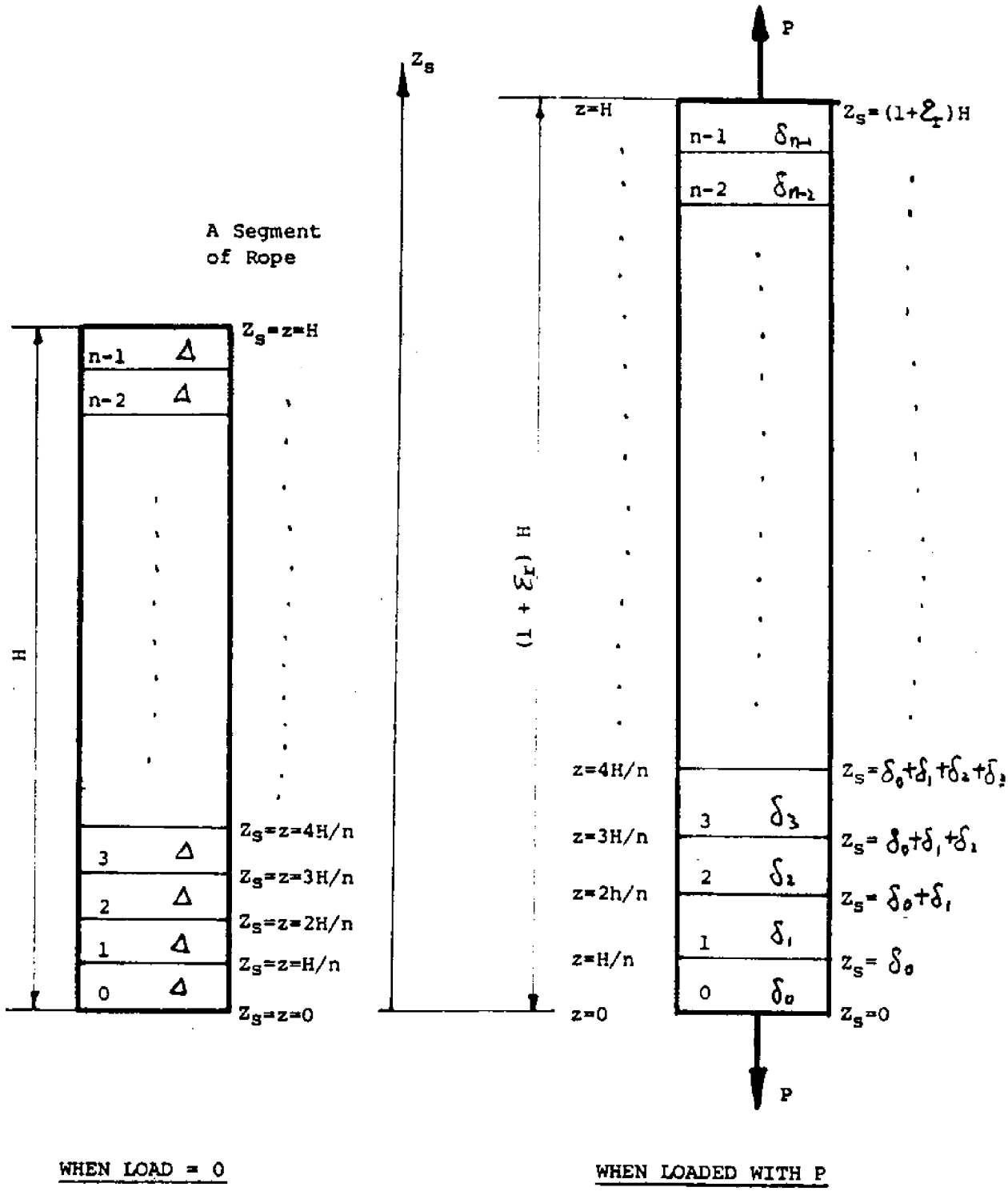

Figure 4: Schematic illustration of a rope segment. (a) before loading (b) Being loaded

with and will move along with the particular cross-section to it. If we measure the new spacing between lines (Figure 4) we may express the spacing as a function of parameter z, and therefore we can define an axial strain function $\epsilon_a(z)$ as:

$$\epsilon_a(z) = \lim_{\Delta \to 0} \frac{\delta(z) - \Delta}{\Delta} = \frac{dZ_s}{dz} - 1 \tag{13}$$

Integrating the above equation once gives:

$$Z_s(z) = \int_0^z [1 + \epsilon_a(z)] dz \tag{14}$$

which is Eq 8.

From the boundary condition, it is necessary that

$$\epsilon_r H = Z_s(H) - H = \text{stretch length} \tag{15}$$

Putting

$$Z_s(H) = \int_0^H [1 + \epsilon_a(z)] dz = H + \int_0^H \epsilon_a(z) dz \tag{16}$$

into Eq 15 gives that:

$$\epsilon_r = \frac{1}{H} \int_0^H \epsilon_a(z) dz \tag{17}$$

which indicates that the average value of the axial strain $\epsilon_a(z)$ must be equal to the rope strain.

Although the exact form of the axial strain function $\epsilon_a(z)$ is determined by the equilibrium condition, it is impossible to find an analytical solution to $\epsilon_a(z)$. However, $\epsilon_a(z)$ can be approximated as close by as desired.

The axial strain function $\epsilon_a(z)$ used in this model is assumed to be a linear function of rope strain and a piecewise linear function of position parameter z, as shown in Figure 5. In the expression for $\epsilon_a(z)$, a_0, a_1, .. a_6 are constants to be

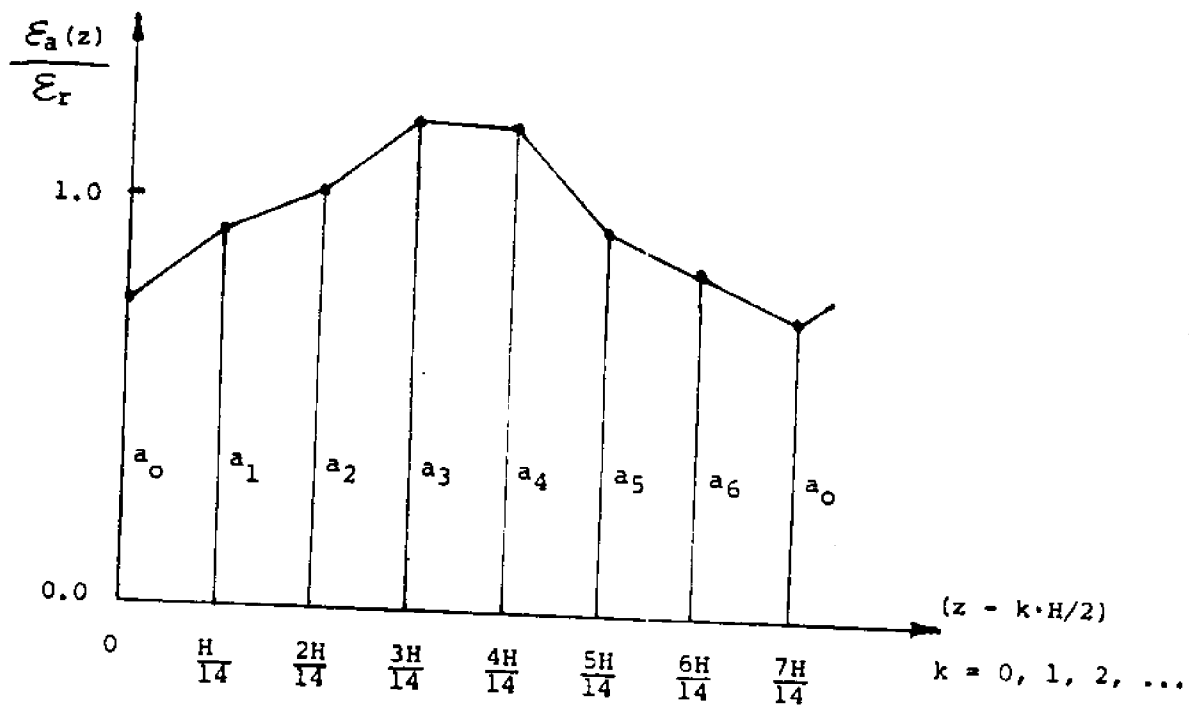

Figure 5: Axial strain function $\epsilon_a(z)$

found (or adjusted) by the model automatically. Due to the structural symmetry of eight-strand ropes, $\epsilon_a(z)$ is a periodic function in z with a period of $H/2$.

The form of axial strain function $\epsilon_a(z)$ shown in Figure 5 has been found to be satisfactory for several eight-strand ropes with different structural parameters, and to be a good compromise between accuracy and computational efficiency. It is possible, however, to further improve the accuracy by dividing $\epsilon_a(z)$ into more pieces of straight lines, and by letting a_i's in $\epsilon_a(z)$ be functions of rope strain instead of being independent of rope strain (i.e. adjust a_i's for each rope strain step).

In this model, the derivatives of strand path functions and strand length are also needed. First, a "dot" operation is defined which denotes taking derivative with respect to the parameter z. Therefore

$$\dot{X}_s \equiv \frac{dX_s}{dz} = X_{max}\frac{2\pi}{H}\cos\frac{2\pi}{H}(z+B) \tag{18}$$

$$\dot{Y}_s \equiv \frac{dY_s}{dz} = -Y_{max}\frac{2\pi}{H}\sin\frac{2\pi}{H}z \tag{19}$$

$$\dot{Z}_s \equiv \frac{dZ_s}{dz} = 1+\epsilon_a(z) \tag{20}$$

Then the derivatives of strand path functions with respect to strand axial coordinate Z_s are given from:

$$\frac{dX_s}{dZ_s} = \frac{dX_s}{dz}\frac{dz}{dZ_s} = \frac{\dot{X}_s}{\dot{Z}_s} \tag{21}$$

$$\frac{dY_s}{dZ_s} = \frac{dY_s}{dz}\frac{dz}{dZ_s} = \frac{\dot{Y}_s}{\dot{Z}_s} \tag{22}$$

The derivative of strand length $S_s(z)$ is given by:

$$\frac{dS_s}{dZ_s} = \frac{dS_s}{dz}\frac{dz}{dZ_s} = \frac{1}{\dot{Z}_s}\frac{dS_s}{dz} \tag{23}$$

By definition, dS_s/dz in above equation can be expressed in terms of $\dot{X}_s$, $\dot{Y}_s$, and $\dot{Z}_s$ as:

$$\frac{dS_s}{dz} = \sqrt{\dot{X}_s^2 + \dot{Y}_s^2 + \dot{Z}_s^2} \tag{24}$$

and the strand length as a function of the parameter z is obtained by integrating Eq 24:

$$S_s(z) = \int_0^z \frac{dS_s}{dz} dz \tag{25}$$

$S_s(z)$ given by Eq 25 cannot be put in the form of an elementary function, and it is evaluated by numerical integration.

The tangential vector of the strand axis will be needed to define the plied yarn path and load calculation. They are given by:

$$T_{sx} = \frac{dX_s}{dZ_s} / \frac{dS_s}{dZ_s} = \dot{X}_s / \frac{dS_s}{dz} \tag{26}$$

$$T_{sy} = \frac{dY_s}{dZ_s} / \frac{dS_s}{dZ_s} = \dot{Y}_s / \frac{dS_s}{dz} \tag{27}$$

$$T_{sz} = \frac{dZ_s}{dZ_s} / \frac{dS_s}{dZ_s} = \dot{Z}_s / \frac{dS_s}{dz} \tag{28}$$

2.2 Geometry of the Plied Yarn Axis

The location of a plied yarn at a given z (the local coordinate) can be found from (Figure 6):

$$\vec{R}_p = \vec{R}_s + \vec{R}'_p \tag{29}$$

where $\vec{R}_p$ and $\vec{R}_s$ are, respectively, the plied yarn path vector and the strand path vector given by:

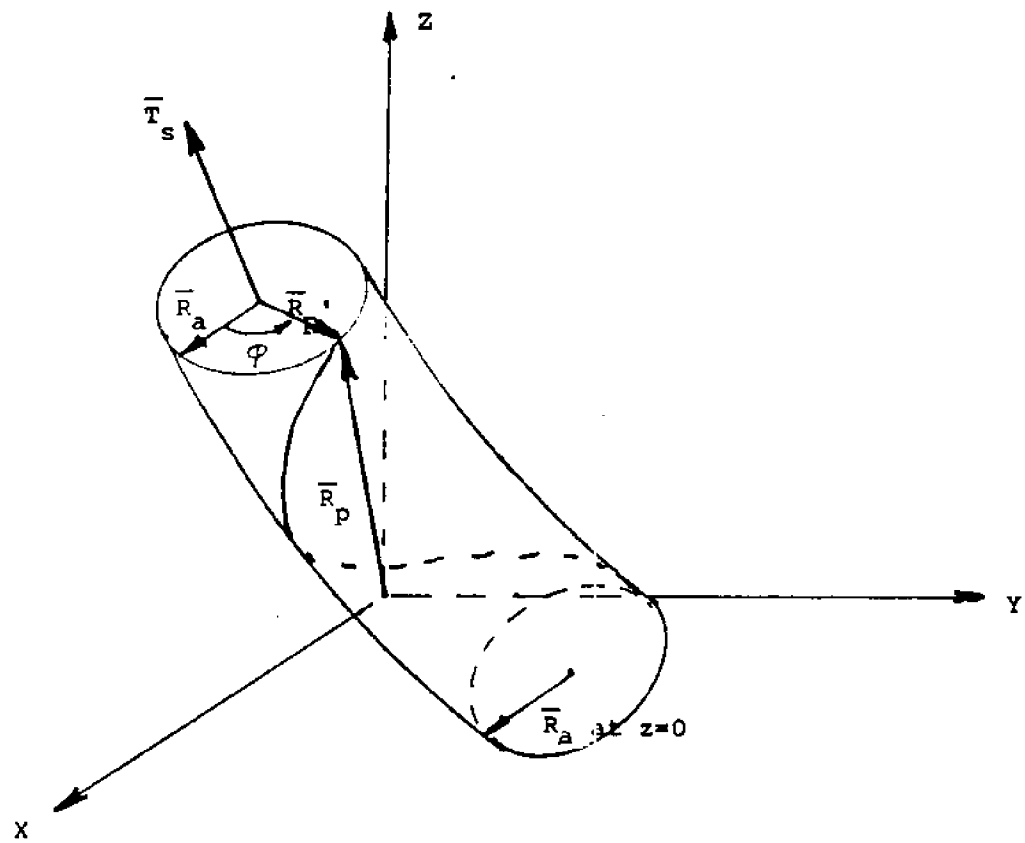

Figure 6: Geometry of the plied yarn axis

$$\vec{R}_p = X_p\vec{i} + Y_p\vec{j} + Z_p\vec{k} \tag{30}$$

$$\vec{R}_s = X_s\vec{i} + Y_s\vec{j} + Z_s\vec{k} \tag{31}$$

and $\vec{R}'_p$ is the relative vector between the plied yarn and the strand axis at given z. Because the plied yarns are twisted around the strand axis to form the strand, the relative vector $\vec{R}'_p$ between a plied yarn and the strand rotates about the strand axis as it moves along the strand axis. In other words, the direction of $\vec{R}'_p$ at a given z can be determined from the plied yarn twist per period of strand, provided that the direction of $\vec{R}'_p$ at $z = 0$ is known. It is also necessary to define a reference direction from which the rotation angle (ϕ) is to be measured, and then to calculate ϕ at that location. Unlike the case of three strand ropes where the normal vector of strand axis pointing to the rope central axis is usually used as the reference vector, the structure of eight-strand ropes does not allow the use of this vector as the reference vector because it is not always pointing to the axis of the rope. In this model, a vector is chosen which is always on the plane perpendicular to Y-axis and on the plane of the strand cross-section, as indicated by the vector $\vec{R}_a$ in Figure 6. The constraints on $\vec{R}_a$, when written in equation forms, are:

$$\vec{R}_a \cdot \vec{j} = 0 \tag{32}$$

and

$$\vec{R}_a \cdot \vec{T}_s = 0 \tag{33}$$

Since the reference vector $\vec{R}_a$ is only used to determine the starting position for measuring the rotation angle ϕ, the magnitude of $\vec{R}_a$ is not important, therefore we may choose:

$$R_{ax} = 1 \tag{34}$$

$$R_{ay} = 0 \tag{35}$$

$$R_{ax} = -\frac{T_{sz}}{T_{sx}} = -\frac{\dot{X}_s}{\dot{Z}_s} \tag{36}$$

to satisfy Eq 32 and 33. Notice that the magnitude of $\vec{R}_a$ thus defined is dimensionless.

The rotation angle ϕ can be calculated from the strand length $S_s(z)$ and the strand twist per period of strand (t) as:

$$\phi(z) = 2\pi t \frac{S_s(z)}{S_s(H)} + \phi_0 \tag{37}$$

where ϕ_0 is the rotation angle ϕ at $z = 0$ and $S_s(H)$ is the strand length per period.

From Figure 6, $\vec{R}_p^l$, the relative vector between the plied yarn and the strand, can be determined from the following three equations:

$$\left|\vec{R}_p^l\right| = r_p \tag{38}$$

$$\vec{R}_p^l \cdot \vec{T}_s = 0 \tag{39}$$

$$\vec{R}_p^l \cdot \vec{R}_a = \cos\phi \tag{40}$$

where r_p is the radius of the plied yarn helix layer. For the eight-strand ropes used in this study, each rope strand consists of nineteen (19) plied yarns located in three layers: the core layer, the sublayer, and the surface layer. If plied yarns are assumed to have circular cross-sections packed concentrically about the strand axis as shown in Figure 7 and each plied yarn is identified by an ID number j given in that figure, the helix radius r_p is seen to be:

$$r_p = \begin{cases} 0 & \text{for core layer } (j = 0) \\ \frac{2}{5}R_s & \text{for sublayer } (1 \le j \le 6) \\ \frac{4}{5}R_s & \text{for surface layer } (7 \le j \le 18) \end{cases} \tag{41}$$

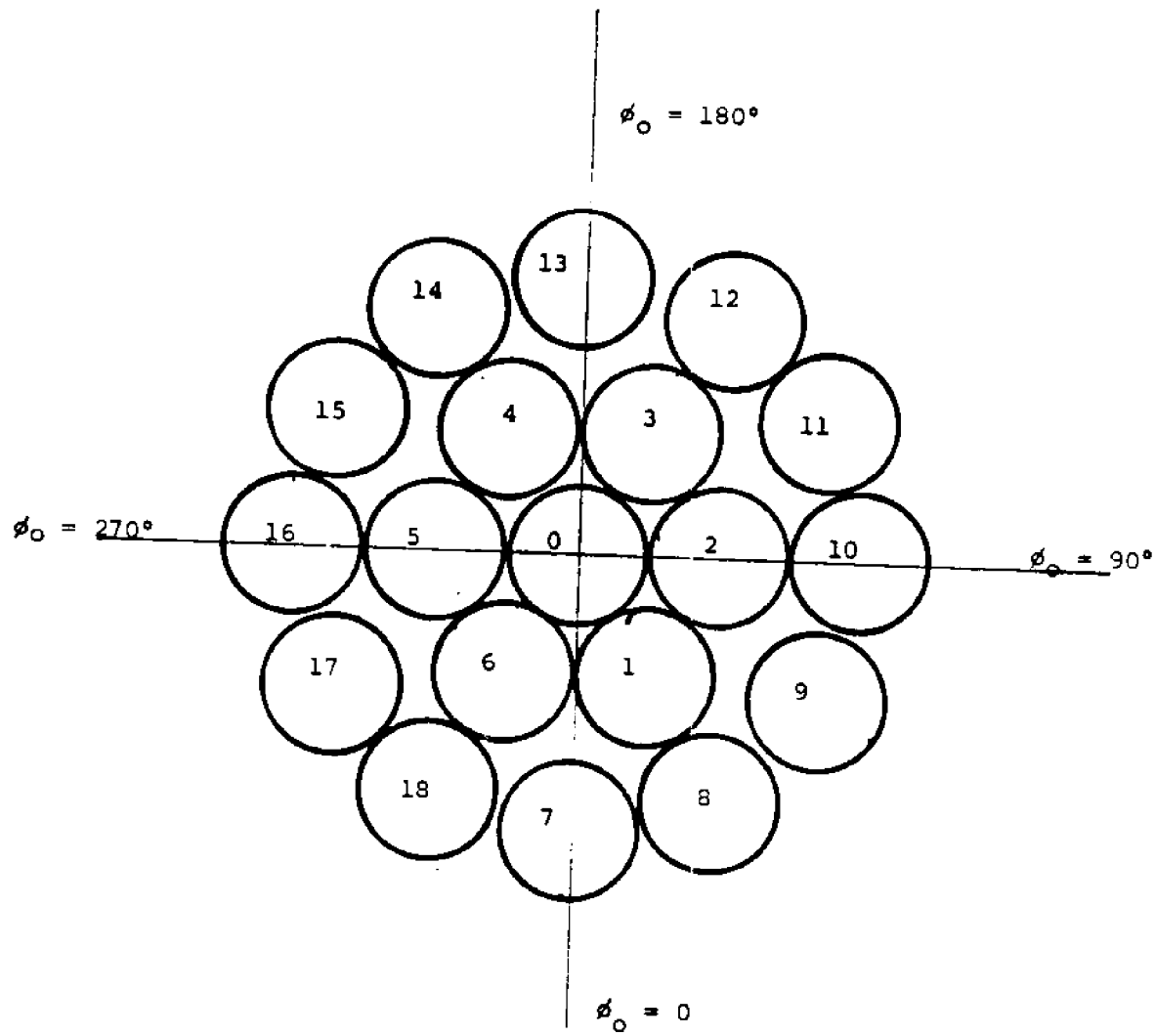

Figure 7: Plied yarn packing pattern across a strand at $z = 0$. Yarn ID number, j, is shown with each yarn.

and the rotation angle (ϕ_0) at $z = 0$ can be calculated as:

$$\phi_0 = \begin{cases} (j-1)\frac{\pi}{3} + \frac{\pi}{6} & \text{for sublayer } (1 \leq j \leq 6) \\ (j-7)\frac{\pi}{6} & \text{for surface layer } (7 \leq j \leq 18) \end{cases} \tag{42}$$

However, these expressions are easily modified to accommodate strand structures with number of plied yarns other than nineteen as in the above case.

From Eq 32–42, the relative vector, $\vec{R}'_p$ can be determined for each plied yarn at any strand cross section indicated by the local coordinate z. Details of such calculation are provided in Appendix A.

After calculating the relative vector $\vec{R}'_p$, the components of the plied yarn position vector $\vec{R}_p$ are calculated according to Eq 29 as:

$$X_p = X_s + R'_{pz} \tag{43}$$

$$Y_p = Y_s + R'_{py} \tag{44}$$

$$Z_p = Z_s + R'_{pz} \tag{45}$$

Notice again that $\vec{R}_p$ is a function of plied yarn ID number, the axial position along the yarn, and the rope strain. It is evaluated numerically then stored in arrays for later use.

Derivatives of the plied yarn coordinates, $\dot{X}_p$, $\dot{Y}_p$, and $\dot{Z}_p$, are calculated using the *Forward Difference Rule* of numerical differentiation which gives an error proportional to the square of the step size Δ for an equation $y = y(x)$:

$$\dot{y}_i = \frac{-y_{i+2} + 4y_{i+1} - 3y_i}{2\Delta} \tag{46}$$

where y_i is the value of y at $x = i\Delta$ and $\dot{y}_i$ is the value of dy/dx at $x = i\Delta$.

The derivative of plied yarn length function $S_p(z)$ is given by:

$$\frac{dS_p}{dz} = \sqrt{\dot{X}_p^2 + \dot{Y}_p^2 + \dot{Z}_p^2} \tag{47}$$

and therefore the plied yarn length per period of strand is:

$$S_p = \int_0^H \frac{dS_p}{dz} dz \tag{48}$$

The X, Y, and Z-components of plied yarn tangential vector $\vec{T}_p$ to be used for load and pressure calculations are given by:

$$T_{px} = \dot{X}_p / \frac{dS_p}{dz} \tag{49}$$

$$T_{py} = \dot{Y}_p / \frac{dS_p}{dz} \tag{50}$$

$$T_{pz} = \dot{Z}_p / \frac{dS_p}{dz} \tag{51}$$

3 ROPE TENSILE BEHAVIOR

3.1 Strain Distributions

When the spatial location of plied yarns as a function of rope strain is defined and available, it is straightforward to calculate the strains across a particular strand cross-section, or the strains along a plied yarn for some limiting cases.

In the case where the friction between plied yarns is neglected, the axial force, and thus the axial strain, of a plied yarn must be constant along the yarn from the consideration of equilibrium. The strain ϵ_p for a given plied yarn at rope strain equal to ϵ_r in this case is simply given by:

$$\epsilon_p = \frac{S_p(\epsilon_r) - S_p(\epsilon_r = 0)}{S_p(\epsilon_r = 0)} \tag{52}$$

where S_p is the plied yarn length per period of strand when the rope is subjected to a strain ϵ_r as indicated in the equation.

The other limiting case is when the friction between plied yarns is so high that no axial relative motions between plied yarns may occur. If we consider an infinitesimal segment of plied yarn ΔS_p in the cylindrical coordinate $\rho\theta z$ system where

$$\rho = \sqrt{X^2 + Y^2} \tag{53}$$

and

$$\tan\theta = \frac{Y}{X} \tag{54}$$

we may express ΔS_p in terms of θ as:

$$\Delta S_p = \frac{dS_p}{d\theta}\Delta\theta \tag{55}$$

where θ is the θ-coordinate in a $\rho\theta z$ system, or called the base angle. For the case of no relative motion between plied yarns, the base angle increment $\Delta\theta$ for the plied yarn segment ΔS_p will remain constant when the rope is stretched. Therefore the local strain for this plied yarn segment is given by:

$$\epsilon_p = \frac{\Delta S_p(\epsilon) - \Delta S_p(\epsilon = 0)}{\Delta S_p(\epsilon = 0)} = \frac{\left.\frac{dS_p}{d\theta}\right|_{\epsilon_r}}{\left.\frac{dS_p}{d\theta}\right|_{\epsilon_r=0}} - 1 \tag{56}$$

Using Chain Rule for differentiation, we have:

$$\frac{dS_p}{dZ_s} = \frac{dS_p}{dz}\frac{dz}{dZ_s} = \frac{dS_p}{dz}\frac{1}{\dot{Z}_s} \tag{57}$$

$$\frac{d\theta}{dZ_s} = \frac{d\theta}{dz}\frac{dz}{dZ_s} = \frac{d\theta}{dz}\frac{1}{\dot{Z}_s} \tag{58}$$

From Eq 54 we have:

$$\frac{d\theta}{dz} = \frac{d[\arctan(Y_s/X_s)]}{dz} = \frac{X_s\dot{Y}_s - \dot{X}_sY_s}{X_s^2 + Y_s^2} \tag{59}$$

where X_s and Y_s are strand path coordinates.

Putting the expressions for X_s, Y_s, $\dot{X}_s$, and $\dot{Y}_s$ derived earlier into Eq 59, it can be seen that $d\theta/dz$ is a function of local coordinate z only, independent of the rope strain ϵ_r. Therefore from Eq 57–59, the plied yarn strain expression Eq 56 may reduce to simply:

$$\epsilon_p = \frac{\left.\frac{dS_p}{dz}\right|_{\epsilon_r}}{\left.\frac{dS_p}{dz}\right|_{\epsilon_r=0}} - 1 \tag{60}$$

Figure 8 shows the plied yarn strain variation across the strand cross-section at $z = 0$, for both cases of no friction between plied yarns and no relative motion between plied yarns. Figure 9 is an illustration of the plied strain variation along plied yarns in different layers of a strand in an eight-strand rope.

3.2 Rope Load-Strain Relations

From the load-extension curve for a tensile test of plied yarns, the modulus of the plied yarns E_p can be found as:

$$E_p = \frac{P_p}{\epsilon_p} \tag{61}$$

where P_p is the plied yarn load at strain ϵ_p.

In general, E_p is a function of plied yarn strain ϵ_p. Although it does not make much difference in the complexity of a numerical model whether E_p is a constant or a complicated function of ϵ_p, we will assume here that E_p is a known constant in the model.

The Z-component of the plied yarn force $P_p(z)$ at a given location z can be calculated from the local plied yarn strain ϵ_p, the Z-component of the plied yarn tangential vector T_{pz} for that yarn, and the plied yarn modulus E_p:

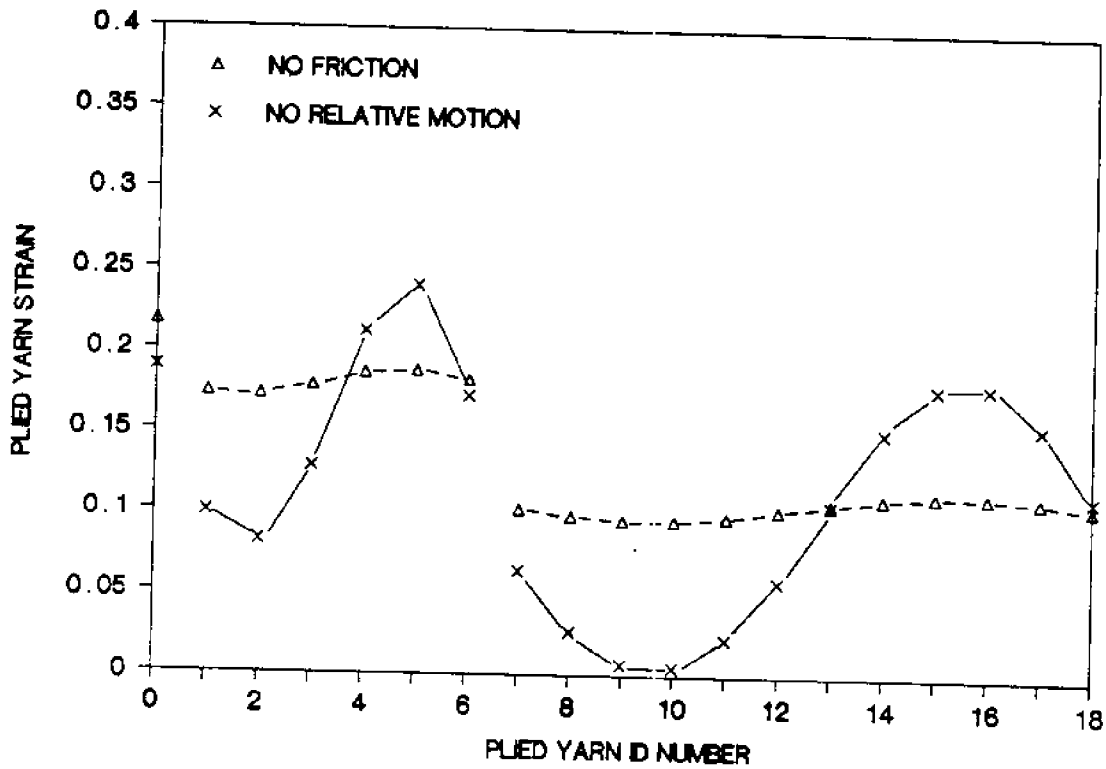

Figure 8: Plied yarn strain variation across the strand ($r_r = 29$ mm, $r_s = 7.5$ mm, $H = 120$ mm, $t = 2.31$ turns/period, $E_p = 11,490$ N/unit strain, $\mu = 0.3$, $z = 0.3$, $\epsilon_r = 0.4$)

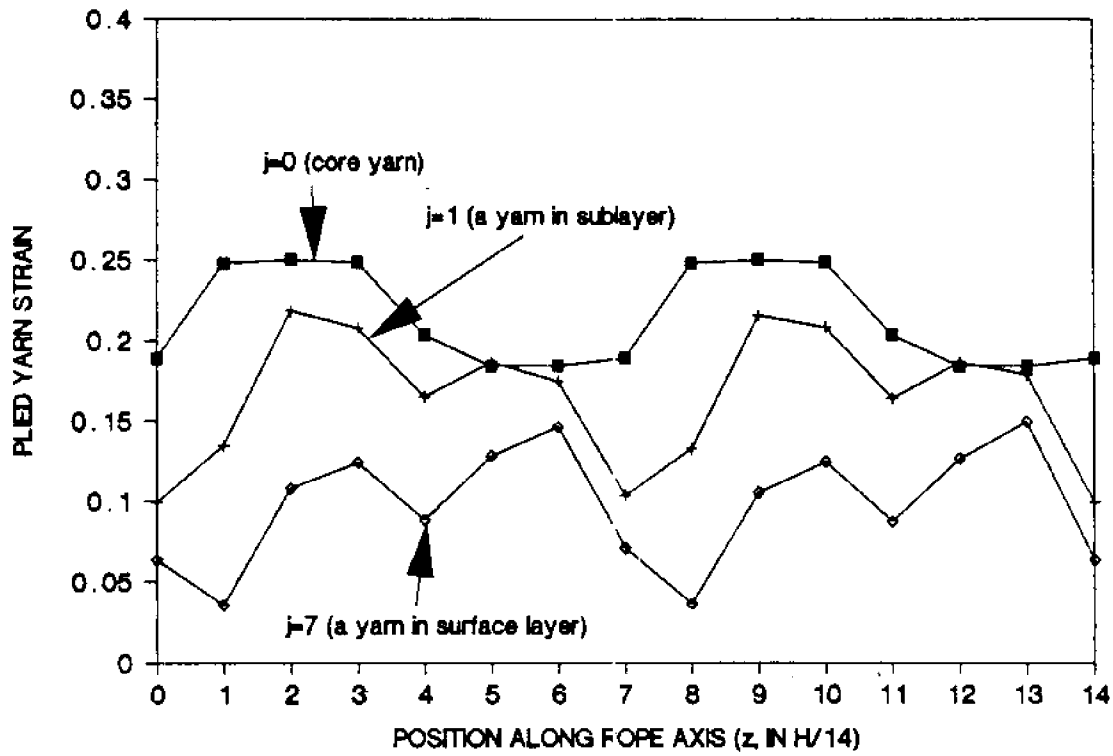

Figure 9: Plied yarn strain variation along plied yarns ($r_r = 29$ mm, $r_s = 7.5$ mm, $H = 120$ mm, $t = 2.31$ turns/period, $E_p = 11{,}490$ N/unit strain, $\mu = 0.3$, $\epsilon_r = 0.4$, no relative motion between plied yarns)

$$P_p(z) = \begin{cases} E_p \epsilon_p T_{ps} & \text{for} \quad \epsilon_p < \epsilon_p^u \\ 0 & \text{for} \quad \epsilon_p \geq \epsilon_p^u \end{cases} \tag{62}$$

where ϵ_p^u is the breaking strain of the plied yarns.

The force in the rope axial direction of a strand at z can be obtained by summing the Z-components of all plied yarn forces in the cross-section:

$$P_s(z) = \sum_{\text{all yarns}} P_p(z) \tag{63}$$

In Eq 62 and 63, it is implicitly assumed that a plied yarn, when strained beyond the breaking point, will not carry any load at that location, and that the breakage will not alter the rope structure by any means. Clearly, these assumptions are not realistic and thus limit this model to the prediction of the rope behavior only up to the initiation of damage due to applied load/stretch. Despite this limitation, the model covers almost the whole range of rope loading/strain of practical interest.

In order to calculate the rope load at a cross-section, we need to know the strand forces in the rope axial direction in that cross-section for all the eight strands. By symmetry, at a cross-section there are four strand pairs in each of which the two strands have the same strain distribution and the same load. By symmetry again, we can find the corresponding locations in the strand we have considered for the four different strands in the cross-section. The rope load $P_r(z)$ is then given by:

$$P_r(z) = 2[P_s(z) + P_s(z + B) + P_s(z + \frac{H}{4}) + + P_s(z + \frac{H}{4} - B)] \tag{64}$$

where B is the phase shift defined in Eq 3, and H is the rope length per period of strand.

As mentioned earlier, the rope load $P_r(z)$ should be constant along the rope axis. In this model, this equilibrium condition is satisfied by proper adjustment of the strand axial strain function, $\epsilon_s(z)$. Details of this adjustment are provided in

Appendix B. Figure 10 and Figure 16 show the load vs. strain characteristics of an eight-strand rope based on three assumed lateral contraction ratios: $\mu = 0.3$, $\mu = 0.6$, and $\mu = 0.3[1 + exp(-\epsilon_r/0.2)]$, for both cases of "no friction" and "no relative motion".

3.3 Inter-Strand Pressures

The spatial configuration of a strand in an eight-strand rope is not in self-equilibrium state, and is supported by other strands via contact stresses. The contact stress, or the inter-strand pressure, is responsible to a great extent for the rope internal abrasion which shortens the life of eight-strand ropes considerably.

Due to the complexity of the structure of eight-strand ropes, it is very difficult to determine the pressure field in an eight-strand rope. However, in most cases we are only interested in certain locations in the rope where high inter-strand pressure is expected. From the rope geometry (see Figure 1 and Figure 2), it is easily seen that the maximum inter-strand pressure occurs near the region where the bending curvature is maximum (i.e. $z = 0$, $H/2$, H, ...). In order to estimate this pressure, we first consider a segment of strand between $z = 1/4H$ and $z = 3/4H$, and determine the resultant force of external pressures on this strand segment, when the rope is stretched. Figure 11 shows the free body diagram of the strand segment under consideration, in which $\vec{R}$ is the resultant force of pressures exerted on the segment, and $\vec{F}_1$ and $\vec{F}_2$ are strand forces at $z = 1/4H$ and $z = 3/4H$ respectively. Force equilibrium requires that:

$$\vec{R} + \vec{F}_1 + \vec{F}_2 = \vec{0} \tag{65}$$

or

$$-R_z = F_{1z} + F_{2z} \tag{66}$$

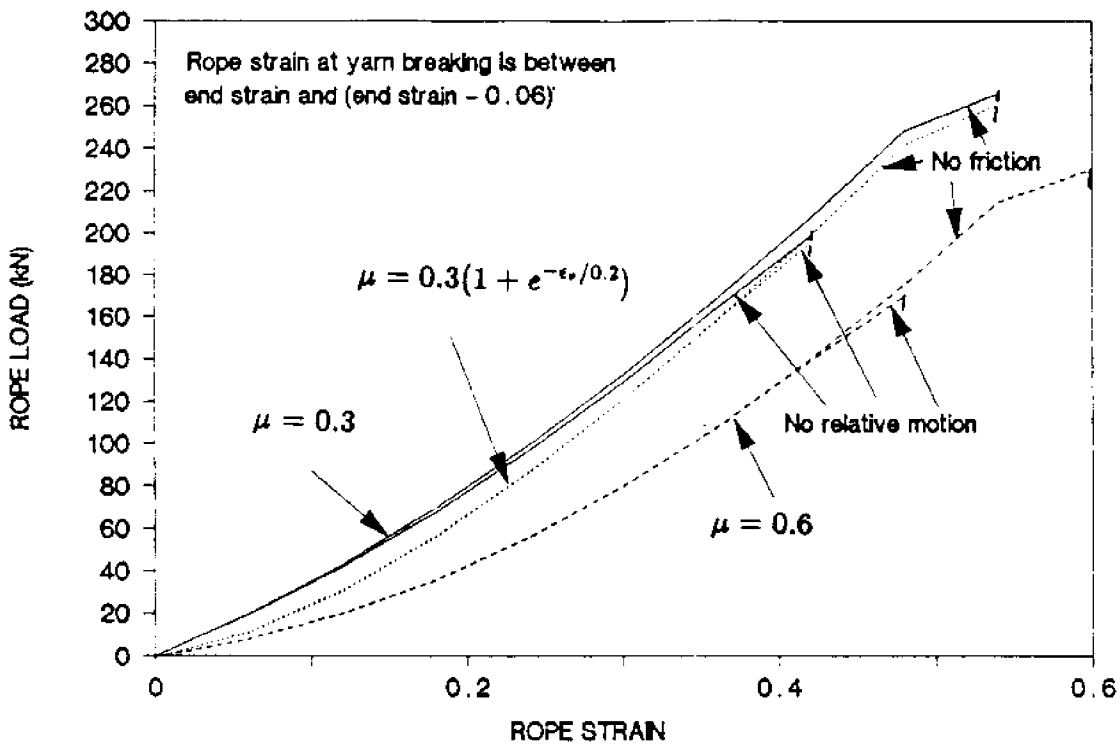

Figure 10: Tensile load vs. strain relationship of eight strand rope ($r_r = 29$ mm, $r_s = 7.5$ mm, $H = 120$ mm, $t = 2.31$ turns/period, $E_p = 11,490$ N/unit strain).

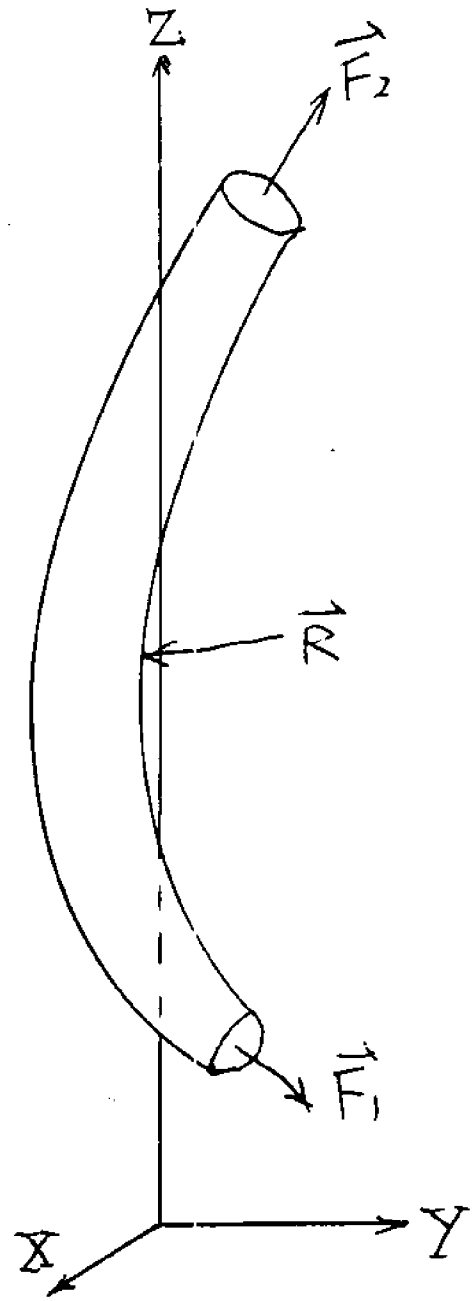

Figure 11: Free body diagram of a strand segment for determination of resultant contact force $\vec{R}$

$$-R_y = F_{1y} + F_{2y} \tag{67}$$

$$-R_x = F_{1x} + F_{2x} \tag{68}$$

In Eq 66, F_{1x}, the x-component of the strand force at $z = 1/4H$, can be calculated directly from the plied yarn strains (ϵ_p), plied yarn modulus (E_p), and the x-component of the local tangential vector of plied yarn path (T_{px}):

$$F_{1x} = \sum_{\text{yarns in strand}} \epsilon_p E_p T_{px} \tag{69}$$

Similar expressions like Eq(78) can be obtained for other components of $\vec{F}_1$ and $\vec{F}_2$.

From the contact force $\vec{R}$, the contact pressure can be calculated if the contact area and the compressive properties of the strand are known. For two isotropic elastic cylinders contacting each other at an angle, the contact area will be an ellipse and the maximum pressure occurs at the center of contact which equals to 1.5 times the average pressure. If this relationship is used to estimate the inter-strand pressure, we will have:

$$p = \frac{1.5P}{\pi ab} \tag{70}$$

where P is the contact (applied) force, (πab) is the contact area with a and b being the minor and major axes of the ellipse.

From the geometry of eight-strand structure, it can be seen that the y-component of the resultant force $\vec{R}$ is primarily supported by the two strands crossing under the strand segment being considered. The contact area is measured from a new rope as approximately $a = 0.5r_s$, and $b = r_s$ where r_s is the strand radius. Therefore the maximum pressure between two crossing strands is given by:

$$p_{\text{crossing}} = \frac{1.5 \cdot 0.5 \cdot R_y}{\pi(0.5R_s)Rs} \tag{71}$$

Similarly it is observed that the x-component of $\vec{F}$ is mainly provided by the strand going parallel to the strand being studied. The contact area for this force component is larger compared with the above case and is roughly given by $a = 0.5r_s$ and $b = 2r_s$. Since this part of strands is on the rope surface, the pressure here will be called "the inter-strand pressure between two parallel strands outside the rope", to distinguish it from the pressure between two parallel strands inside the rope. The maximum pressure between two parallel strands outside the rope is determined from:

$$p_{\text{parallel, outside}} = \frac{1.5R_z}{\pi(0.5R_s)(2R_s)} \tag{72}$$

Another region with high inter-strand pressure, as mentioned earlier, is between two parallel strands inside the rope which support the strand analyzed above. The contact force between two parallel strands inside the rope can be estimated by considering a segment of strand between $z = 1/4H$ and $3/4H$, on which the forces have been determined, and the two strands under it. Figure 12 shows the simplified force-equilibrium diagram, from which the contact force due to one crossing strand is approximately given by:

$$F_{\text{contact}} = 0.5R_y \cdot T_{zz}|_{z=1.5R_s/\sin\gamma} \tag{73}$$

Note that there are actually two strands going above the two strands inside the rope, therefore the contact force is twice as large as that given by Eq(82). If we again assume the contact area is an ellipse with $a = r_s$ and $b = 4r_s$, then the inter-strand pressure between two parallel strands inside the rope is:

$$p_{\text{parallel, inside}} = \frac{1.5 \cdot 2 \cdot 0.5R_y \cdot T_{zz}}{\pi(0.5R_s)(2R_s)} \tag{74}$$

The inter-strand pressures between crossing and parallel strands are plotted in Figure 13, Figure 14 and Figure 15 as functions of the rope strain.

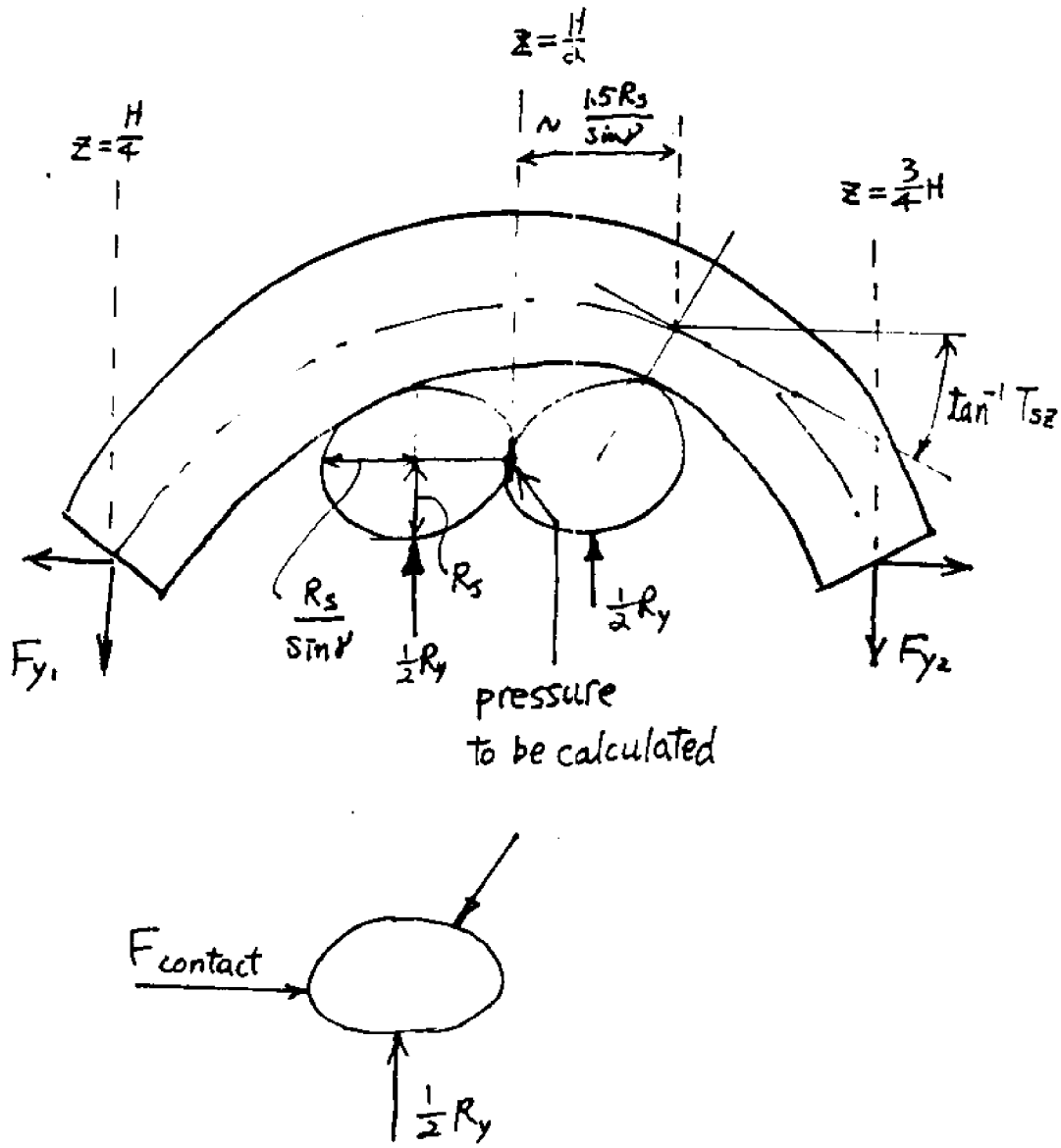

Figure 12: Simplified equilibrium diagrams for the contact forces. γ is the angle between the two sets of crossing strands.

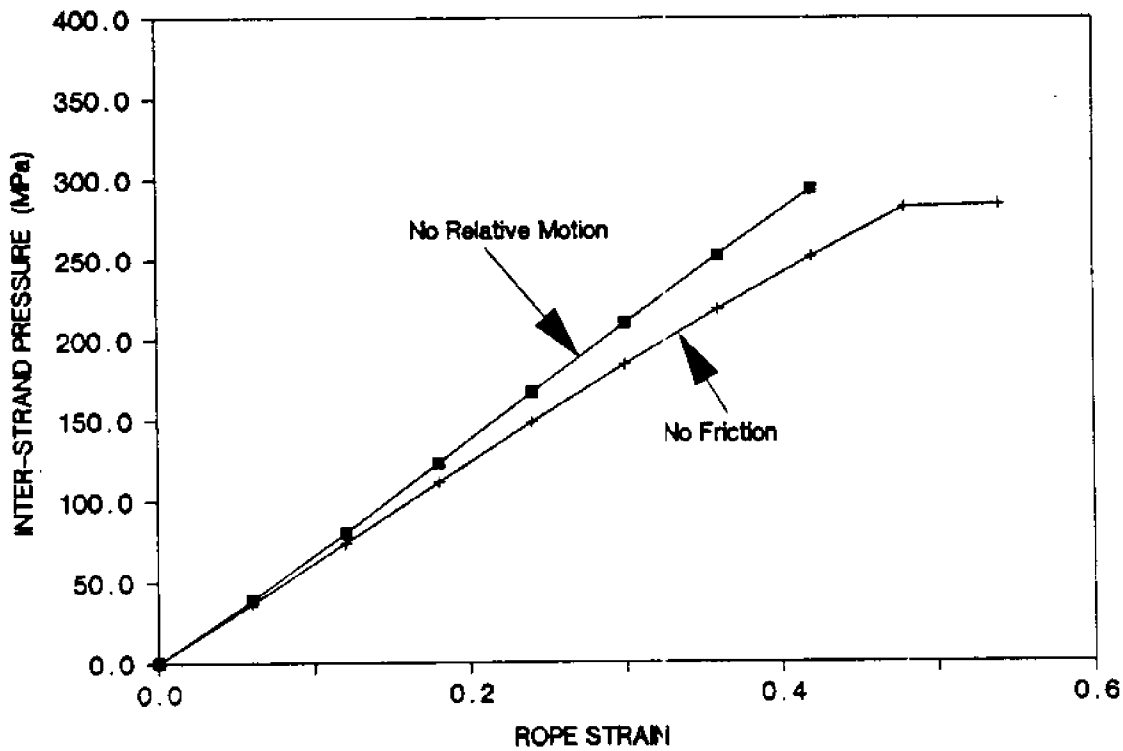

Figure 13: Inter-strand pressure between crossing strands. ($r_r = 29$ mm, $r_s = 7.5$ mm, $H = 120$ mm, $t = 2.31$ turns/period, $E_p = 1.1,490$ N/unit strain, $\mu = 0.3$).

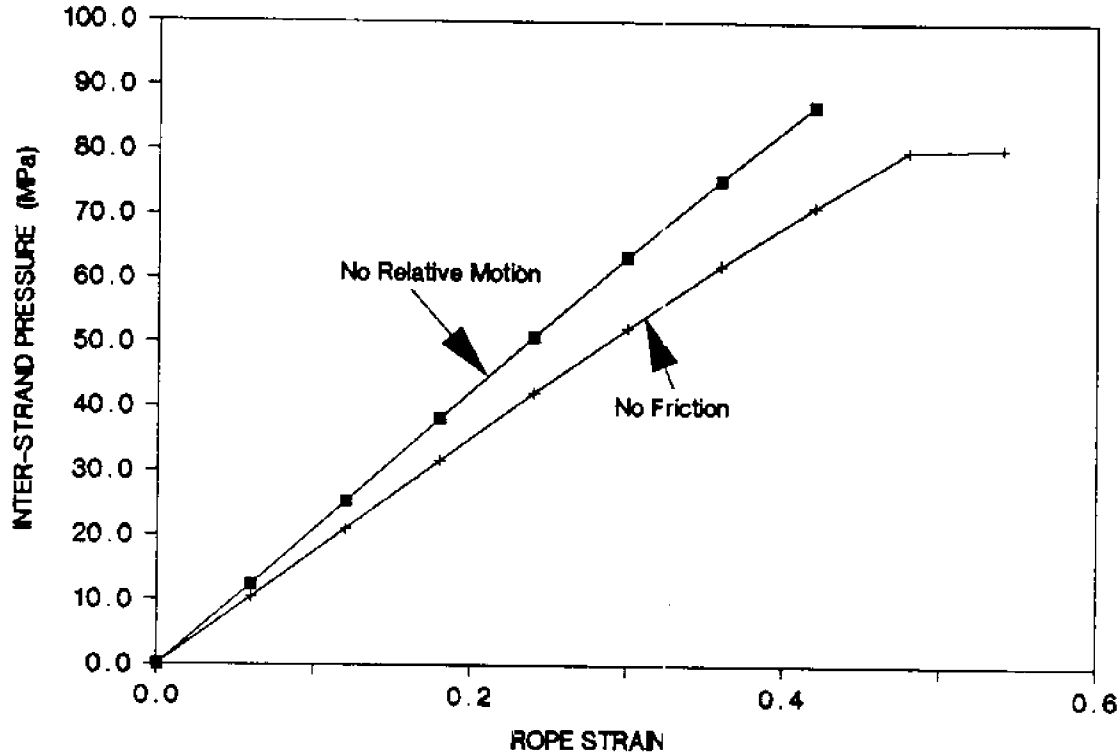

Figure 14: Inter-strand pressure between parallel strands outside rope. (r_r = 29 mm, r_s = 7.5 mm, H = 120 mm, t = 2.31 turns/period, E_p = 11,490 N/unit strain, μ = 0.3).

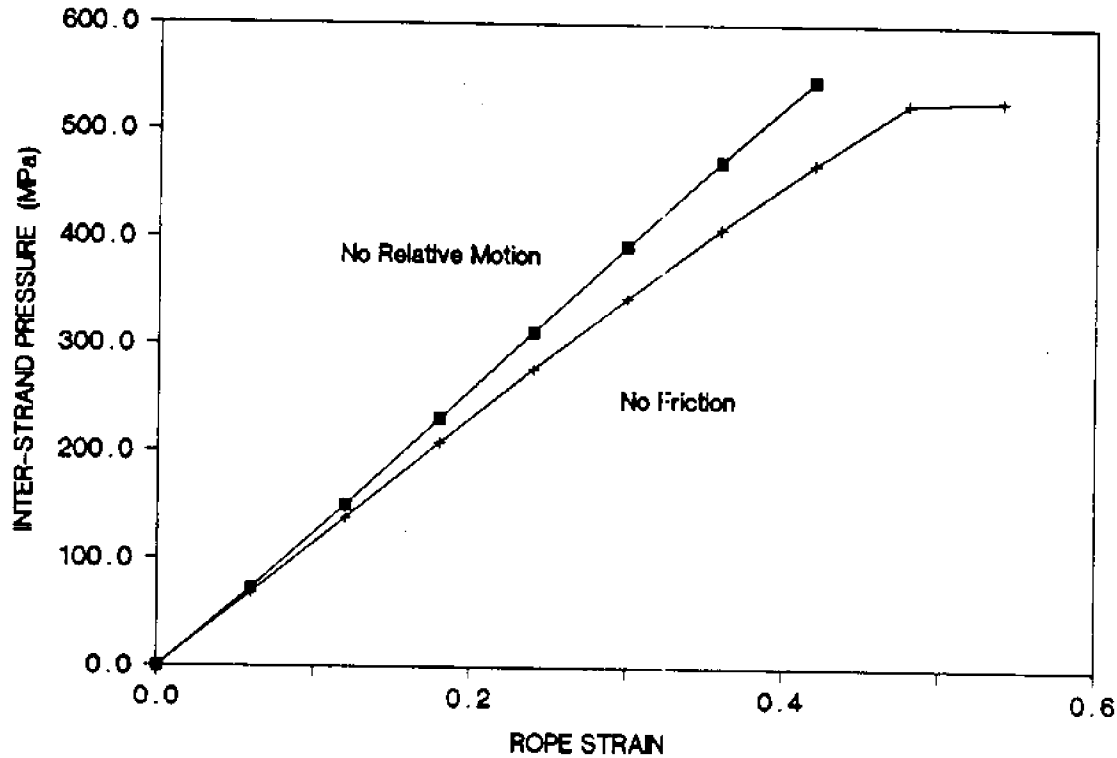

Figure 15: Inter-strand pressure between parallel strands inside rope. (r_r = 29 mm, r_s = 7.5 mm, H = 120 mm, t = 2.31 turns/period, E_p = 11,490 N/unit strain, $\mu = 0.3$).

It can be seen that very high pressures are built up in eight-strand ropes, especially between crossing strands and between parallel strands inside the rope, which cause severe wear damage to such rope when subjected to cyclic tensioning.

3.4 Relative Slippages between Strands

The relative slippage distance between strands is as important as the inter-strand pressures, as both are responsible for the internal abrasion of eight-strand ropes. Generally the relative slippage between strands can be considered as composed of two basic relative motions: strand sliding on each other, and strand rotation about different pivoting points. Because of the symmetrical property of eight-strand ropes, the slippage due to strand relative sliding is not expected in certain rope cross-sections. In the regions where high inter-strand pressures occur as considered in the previous section, the relative slippage is mainly due to the strand rotation.

Figure 16 is a sketch showing the directions of four strands in a rope, in which α and β are the directional angle between strand axes and the Z-axis, at the location as shown. When the rope is stretched, both α and β will change as functions of rope strain, causing relative slippage between crossing strands as well as parallel strands. α and β are determined from:

$$\alpha = \arctan \left. \frac{\partial X_s}{\partial Z_s} \right|_{s=0} \tag{75}$$

$$\beta = \arctan \left. \frac{\partial Y_s}{\partial Z_s} \right|_{s=H/4} \tag{76}$$

The relative slippage distance between two parallel strands outside the rope is approximately:

$$\delta_{\text{parallel, outside}} = 2r_s \sin(\alpha_0 - \alpha) \tag{77}$$

Figure 16: Directions of strand axes at an intersection

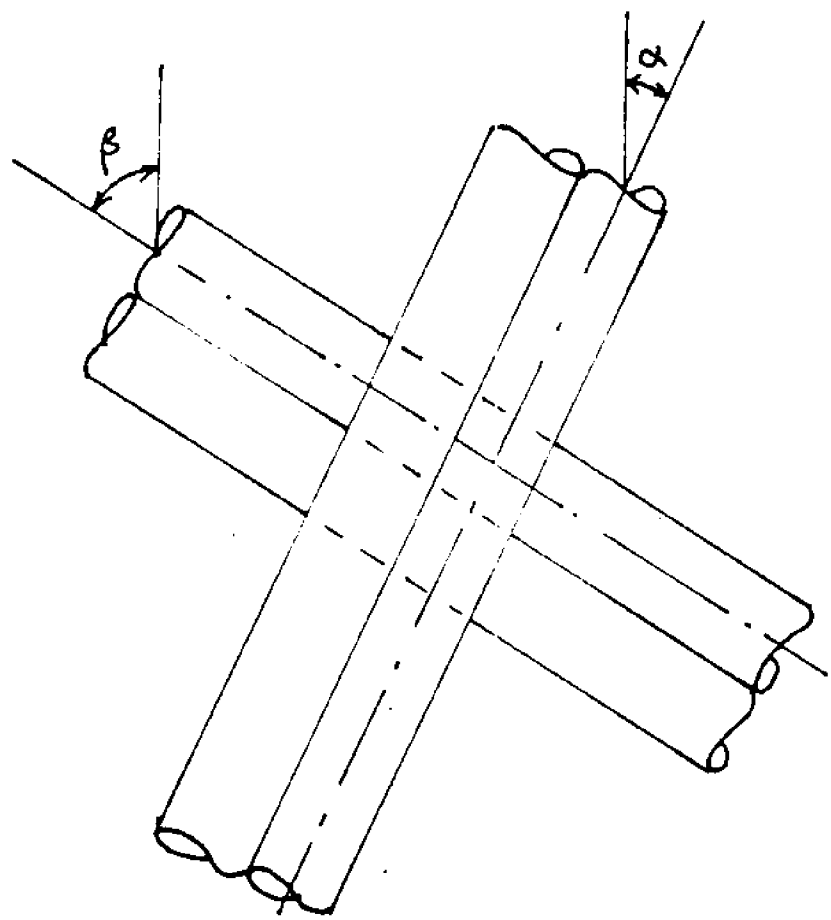

the relative slippage distance between two parallel strands inside the rope is:

$$\delta_{\text{parallel, inside}} = 2r_s \sin(\beta_0 - \beta) \tag{78}$$

and the relative slippage distance between the crossing strands is given as:

$$\delta_{\text{crossing}} = 2r_s[(\alpha_0 + \beta_0) - (\alpha + \beta)] \tag{79}$$

where α_0 and β_0 are the corresponding α and β values when rope is not stretched. These slippage distances are plotted in Figure 17.

4 DISCUSSION AND CONCLUSIONS

A structural model for eight strand rope has been established which describes the geometric locations of the rope strands and the plied yarns in each strands, both at load free state as well as when the rope is subjected to tensile stretch. Relative slippage between strands resulted from the geometric change is evaluated as a function of rope strain. Plied yarn local strains are also calculated from the geometric change due to loading for two limiting cases: (1) assume that there is no friction between plied yarns in a rope strand, and (2) assume that the friction between plied yarns in a strand is sufficiently large to prevent any relative motion between adjacent plied yarns. As these assumptions imply, strains along plied yarns for the no friction case are constant, and they vary along the yarns for the case of no relative motion. The average strain decreases from the core to the sublayer and to the surface layer.

Rope load vs. strain relations are determined from the plied yarn strain distribution and the tensile behavior of plied yarns. Similar tensile behavior is predicted regardless the assumption of no friction or no relative motion. However, the rope breaking strain or load depends on such assumption — the rope breaks at a smaller strain (or load) for the case of no relative motion due to the strain variation in plied yarns.

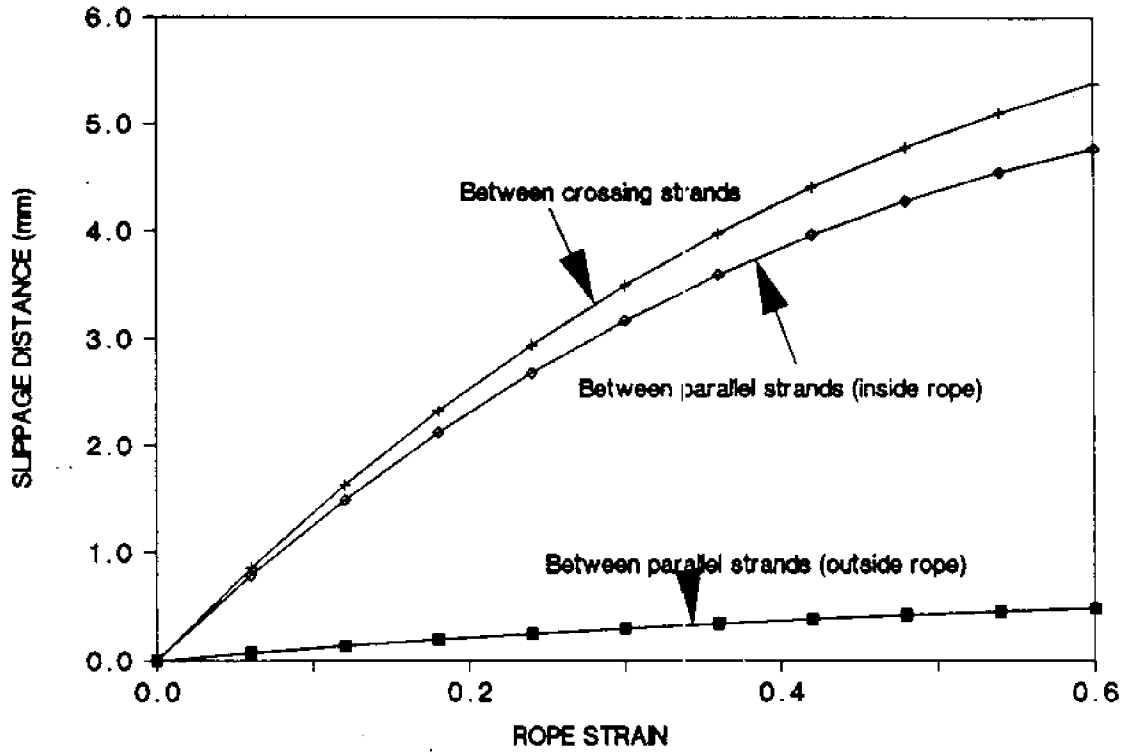

Figure 17: Relative slippage distances between strands. ($r_r = 29$ mm, $r_s = 7.5$ mm, $H = 120$ mm, $t = 2.31$ turns/period, $E_p = 11,490$ N/unit strain, $\mu = 0.3$).

Contact pressures between strands are estimated from the rope strand forces. Highest inter strand pressure occurs between two parallel strands in side the rope, and between two sets of crossing strands. These areas of high interstrand pressure are also where significant amount of slippage between strands takes place as the rope is stretched. Heavy abrasion at these areas is thus expected when the rope is subjected to cyclic loads, and indeed significant abrasion can be found there in eight strand ropes after deployment.

The rope tensile behavior is also strongly influenced by the assumed value of rope lateral contraction ratio, μ. Until a satisfactory method of determination of μ is found and used in the model, the results of this model can only be considered qualitative. But nonetheless, the model can be used to study the dependency of rope tensile behavior on other parameters and used as guideline for the design of more efficient ropes.

A Determination of Relative Vector $\vec{R}'_p$

For the case of $\dot{Y}_s = 0$, which means both $\vec{R}_a$ and $\vec{T}_s$ vectors are on the XOZ plane and are perpendicular to the Y-axis as shown in Figure 18, $\vec{R}'_p$ can be directly calculated by referring to the figure:

$$R'_{px} = (r_p \cos\phi)\frac{\vec{R}_a \cdot \vec{i}}{|\vec{R}_a|} = \frac{r_p \cos\phi}{|\vec{R}_a|} \tag{80}$$

$$R'_{py} = r_p \sin\phi \tag{81}$$

$$R'_{pz} = (r_p \cos\phi)\frac{\vec{R}_a \cdot \vec{k}}{|\vec{R}_a|} = -\frac{\dot{X}_s r_p \cos\phi}{\dot{Z}_s |\vec{R}_a|} \tag{82}$$

For the general case when $\dot{Y}_s \neq 0$, we first rewrite Eq 38–40 in an equivalent but more workable form:

$$(R'_{px})^2 + (R'_{py})^2 + (R'_{pz})^2 = r_p^2 \tag{83}$$

$$R'_{px}\dot{X}_s + R'_{py}\dot{Y}_s + R'_{pz}\dot{Z}_s = 0 \tag{84}$$

$$R'_{px} - R'_{pz}\frac{\dot{X}_s}{\dot{Z}_s} = |\vec{R}_a| r_p \cos\phi \tag{85}$$

Then we can solve for R'_{px} and R'_{py} in terms of R'_{pz} from Eq 84 and 85:

$$R'_{px} = |\vec{R}_a| r_p \cos\phi + R'_{pz}\frac{\dot{X}_s}{\dot{Z}_s} \tag{86}$$

$$R'_{py} = -\left[\frac{\dot{X}_s}{\dot{Z}_s}|\vec{R}_a| r_p \cos\phi + (1 + \frac{\dot{X}_s^2}{\dot{Z}_s^2})R'_{pz}\right]\frac{\dot{Z}_s}{\dot{Y}_s} \tag{87}$$

Putting Eq 86 and 87 into Eq 83 yields a quadratic equation in R'_{pz}:

$$A(R'_{pz})^2 + BR'_{pz} + C = 0 \tag{88}$$

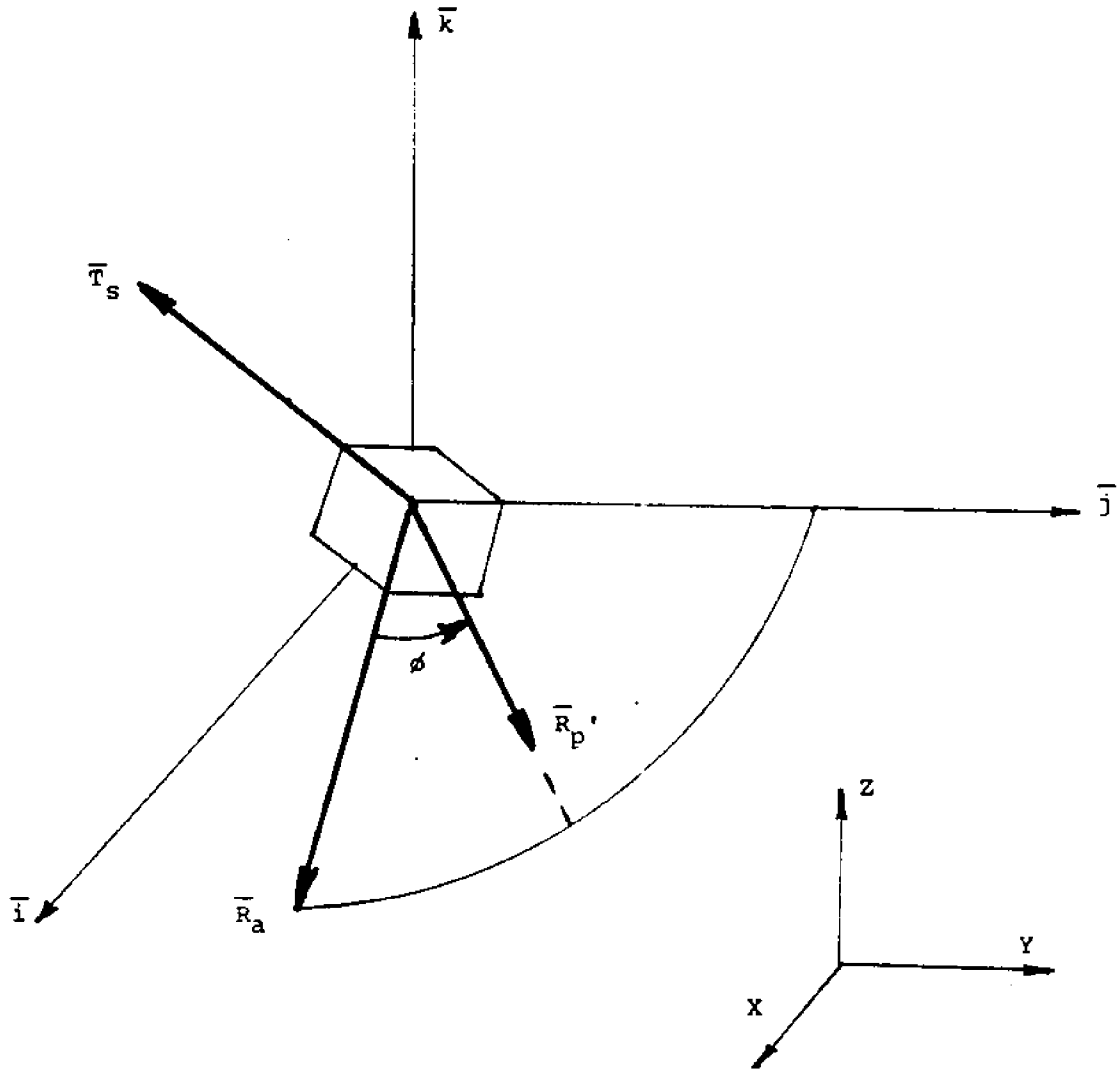

Figure 18: Determination of $\vec{R}_p$ for the case of $\dot{Y}_s = 0$

with:

$$A = \left(\frac{\dot{X}_s}{\dot{Z}_s}\right)^2 + \left(\frac{\dot{X}_s^2 + \dot{Z}_s^2}{\dot{Y}_s \dot{Z}_s}\right)^2 + 1$$

$$B = 2\frac{\dot{X}_s}{\dot{Z}_s}\left(1 + \frac{\dot{X}_s^2 + \dot{Z}_s^2}{\dot{Y}_s^2}\right)|\vec{R}_a| r_p \cos\phi$$

$$C = \left(1 + \frac{\dot{X}_s^2}{\dot{Y}_s^2}\right)(|\vec{R}_a| r_p \cos\phi)^2 - r_p^2$$

Letting

$$D = \sqrt{B^2 - 4AC} \tag{89}$$

R'_{ps} is readily calculated from:

$$R'_{ps} = \frac{-B \pm D}{2A} \quad \text{for } \dot{Y}_s \neq 0 \tag{90}$$

if the sign before D is properly set. Determination of the sign before D in Eq 90 is discussed in detailed as follows.

To derive an equation for determining the sign for the determinant D in Eq 90, we first go back to Eq 38–40 from which $\vec{R}'_p$, the relative vector between the plied yarn position vector ($\vec{R}_p$) and the strand position vector ($\vec{R}_s$), is to be found. It can be seen that these equations are only the necessary conditions for determining $\vec{R}'_p$, not sufficient conditions and therefore the solution of $\vec{R}'_p$ to these equations is not unique. Because of the even property of a cosine function, the mirror image of $\vec{R}'_p$ in the same strand cross-section about the reference vector $\vec{R}_a$ also satisfies Eq 38–40 as does $\vec{R}'_p$. The $\vec{R}'_p$ shown in Figure 6 corresponds to a positive rotation angle ϕ (the plied yarn is right-hand twisted), while its mirror image corresponds to a negative ϕ (the plied yarn is left-hand twisted). Of course, for a given rope strand there can only be one direction of plied yarn twist about the strand axis. In the

rope manufacturing industry, the direction of plied yarn twist about the strand axis is always opposite to that of strand twist about the rope axis, in order to increase the strength efficiency and geometric stability of ropes. Since the one rope strand picked up to model happens to be left-hand twisted about the rope axis, the plied yarn twist should be in right-hand direction, indicating that the relative vector $\vec{R}'_p$ corresponding to a positive ϕ shown in Figure 6 is the one that we are interested in. Unfortunately, both $\vec{R}'_p$ and its mirror image are given by the same set of equations (Eq 86–90), and they are not easily separatable.

Figure 19 is a plot of the Z-component of $\vec{R}'_p$ (R'_{pz}) for a plied yarn calculated from Eq 90 when both "+" and "-" signs in the equation are used. Clearly we can see that using "+" or "-" sign alone in Eq 90 will not give a result that makes sense. However, if we shift the sign before D in Eq 90 properly, we may get two smooth curves for R'_{pz} , as shown in Figure 20a and Figure 20b, directly from Figure 19. The "shift" seems very unpredictable, but it can be shown that we can get the Z-component of $\vec{R}'_p$, plotted in Figure 20a, from Eq 90 if we use the following formula to select the sign before D in that equation:

$$\text{Sign} = (-1)^{m+1} \frac{\dot{Y}_s(z)}{|\dot{Y}_s(z)|} \tag{91}$$

where $m \equiv [\phi/\pi]$, the integer part of ϕ/π. The sign is just the opposite for the mirror image of $\vec{R}'_p$ (Figure 20b). Although the derivation of Eq 91 is not simple, one can easily prove it by plotting the components of $\vec{R}'_p$ for each plied yarn using this rule to see whether the resulting $\vec{R}'_p$ is a smooth function of position parameter z.

Once the sign for D in Eq 90 is found, the three components of $\vec{R}'_p$, R'_{px}, R'_{py}, and R'_{pz}, can then be obtained from Eq 86, 87, and 90. Figure 21 shows the variation of the components of $\vec{R}'_p$ as functions of parameter z for a plied yarn (Yarn 7 in Figure 7) right-hand twisted about the rope axis (Figure 6).

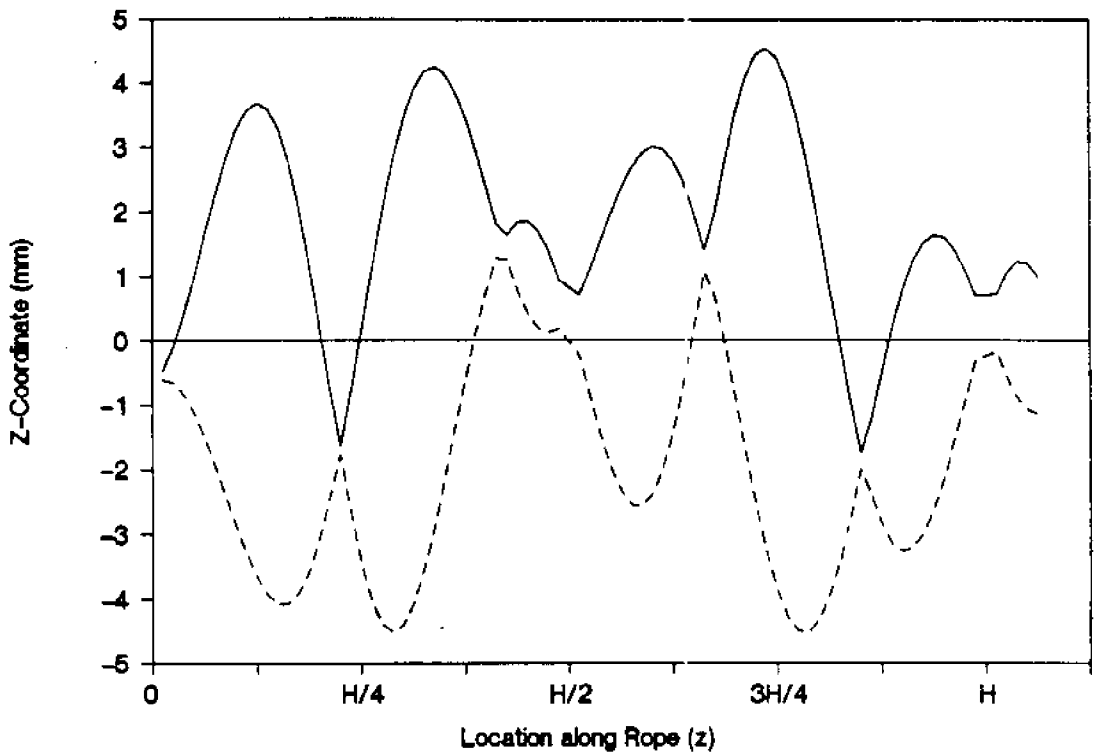

Figure 19: R'_{pz} as determined from Eq 90. Solid line is computed from $R'_{pz} = (-B + D)/2A$ and broken line from $R'_{pz} = (-B - D)/2A$.

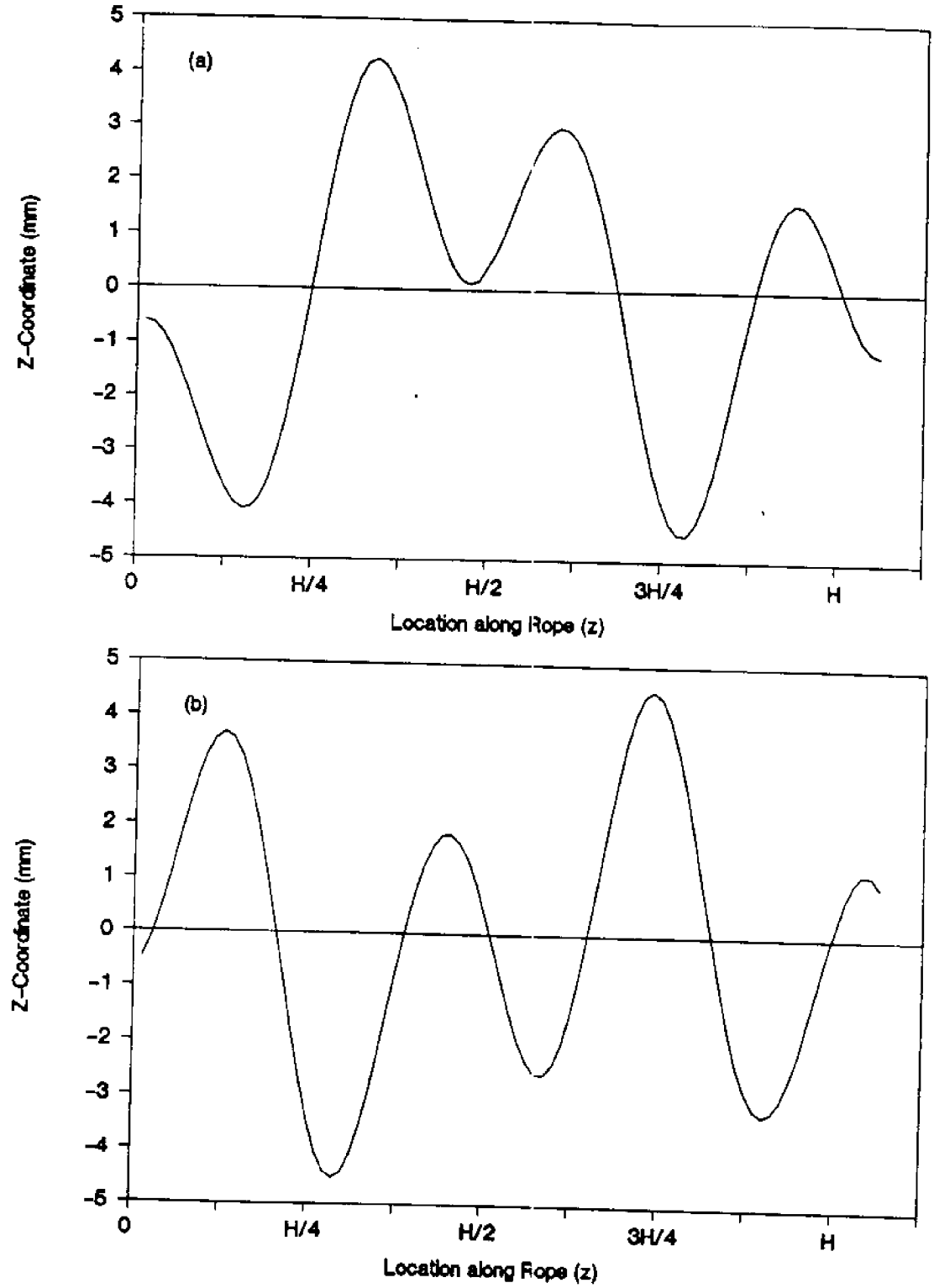

Figure 20: Two smooth curves for R'_{ps}

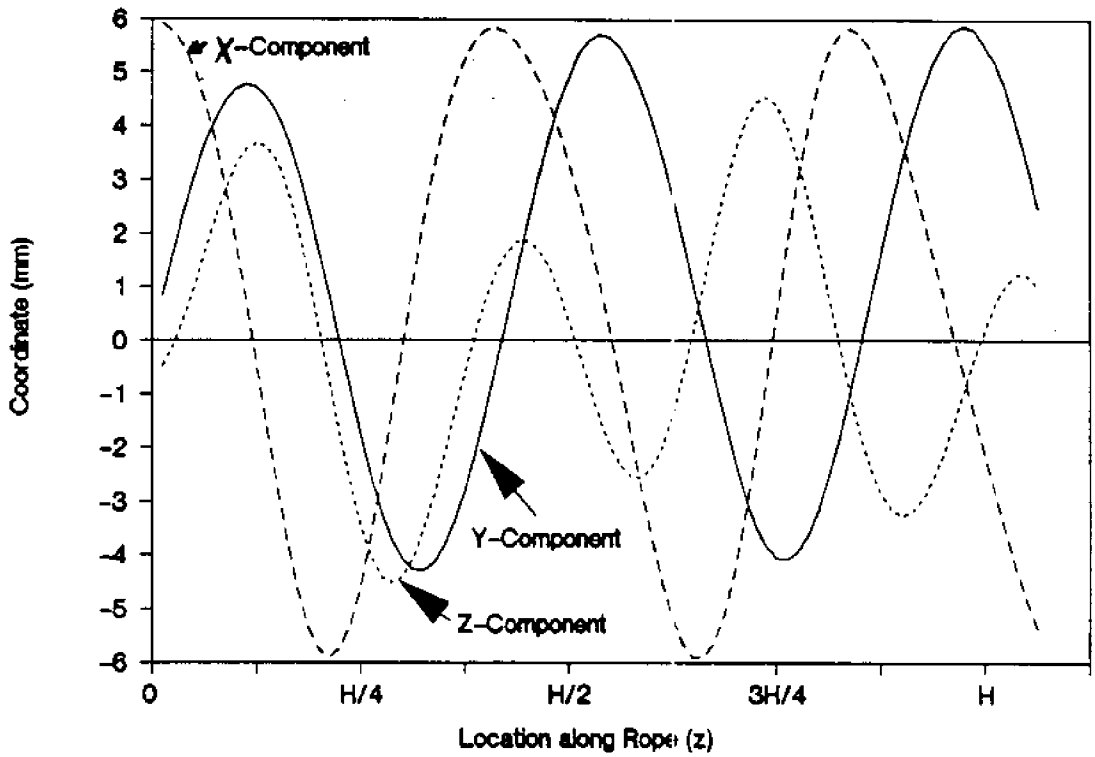

Figure 21: Components of $\vec{R}'_p$ as a function of z

B Adjustment of $\epsilon_a(z)$

The rope load $P_r(z)$ should be constant along the rope axis. However, it is impossible, and probably not necessary, to make the rope load P_r be exactly the same in all rope cross-sections. In order to control the load variation along the rope axis, seven cross-sections within the range of $z = 0$ and $z = H/2$ are chosen to calculate the rope loads ($\epsilon_a(z)$ is assumed to be periodic with a period of $H/2$ in z). The load variation is only checked for one rope strain level to increase the calculation speed. Coefficient of variation (CV, the standard deviation divided by the average) of rope loads in these cross-section is calculated from:

$$CV = \frac{\sqrt{\frac{\sum P_{ri}^2}{n-1} - \frac{(\sum P_{ri})^2}{n(n-1)}}}{\frac{\sum P_{ri}}{n}} \tag{92}$$

where P_{ri} is the rope load at i-th cross-section, n is the number of cross-sections considered ($n = 7$ here), and all the summations are over $i = 0$ to $i = 6$.

If the calculated CV is within the range of acceptance (say, less than 3%) indicating the validity of the model, complete calculation of the plied yarn strain distribution and rope load for a range of rope strains is proceeded. Otherwise if the CV is not acceptable, the axial strain function $\epsilon_a(z)$ is modified by adjusting its parameters according to the currently calculated loads P_{ri}'s:

$$a_i|_{\text{new}} = \left[1 + 5CV\left(\frac{\bar{P}_r}{P_{ri}} - 1\right) + CV\left(\frac{\bar{P}_r}{P_{r(i-1)}} - 1\right)\right] a_i|_{\text{old}} \tag{93}$$

where a_i is the axial strain $\epsilon_a(z)$ at the i-th cross-section as defined in Figure 5, CV is the coefficient of variation of rope loads in different sections, and $\bar{P}_r$ is the average rope load.

With the modified axial strain function, loads are recalculated and if necessary the strain function is re-modified, until the given criterion is met. This algorithm of

finding the axial strain function $\epsilon_a(z)$ has been tested for different rope parameters to result in a rope load variation within 2% for the rope strain it based on.